Report

Contribution of Temperature Increase to Restrain the Transmission of COVID-19

Mengyuan Ren,[1,2,11] Rongjuan Pei,[3,11] Bahabaike Jiangtulu,[1,2,11] Junxi Chen,[1,2,11] Tao Xue,[1,2] Guofeng Shen,[4] Xiaoru Yuan,[5] Kexin Li,[6] Changxin Lan,[1,2] Zhen Chen,[3] Xinwen Chen,[3] Yun Wang,[3] Xiaoqian Jia,[1,2] Zewu Li,[1,2] Audil Rashid,[7] Tippawan Prapamontol,[8] Xiuge Zhao,[9] Zhaomin Dong,[10] Yali Zhang,[1,2] Le Zhang,[1,2] Rongwei Ye,[1,2] Zhiwen Li,[1,2] Wuxiang Guan,[3,*] and Bin Wang[1,2,*]
*Correspondence: guanwx@wh.iov.cn (W.G.); binwangpku@foxmail.com (B.W.)
Received: August 11, 2020; Accepted: December 12, 2020; Published Online: December 15, 2020; https://doi.org/10.1016/j.xinn.2020.100071

GRAPHICAL ABSTRACT

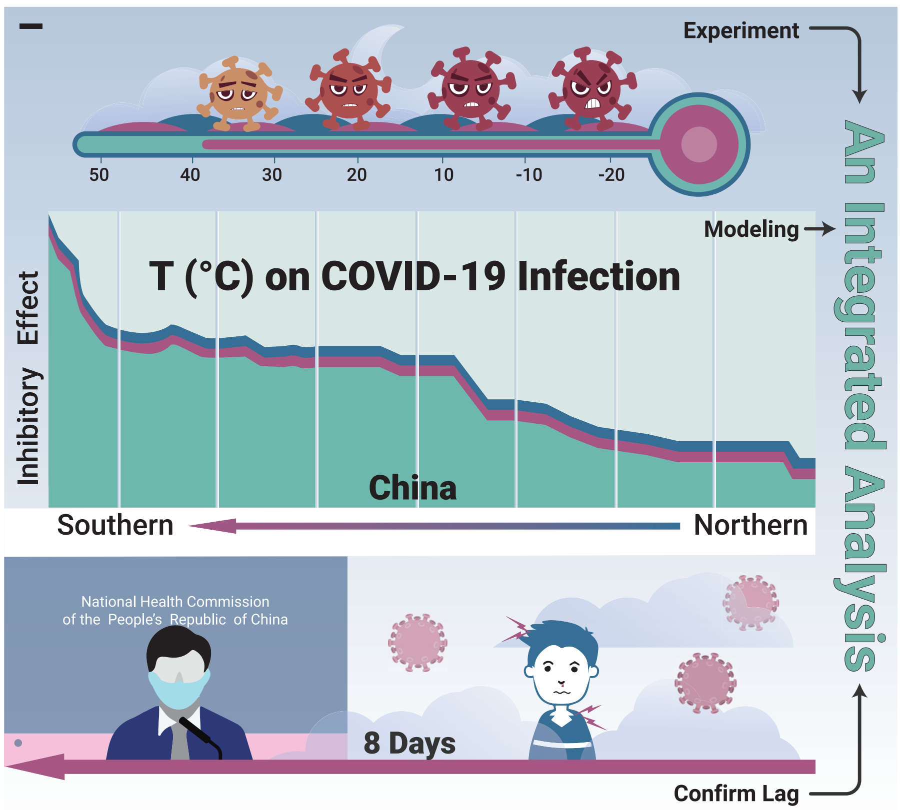

PUBLIC SUMMARY

- Temperature increase was associated with restrained transmission of COVID-19 on the Chinese Mainland
- The above association was estimated to be strongest when the lag time from SARS-CoV-2 infection to the official confirmation report was 8 days
- In geographical regions without central heating, temperature increase had a stronger effect on restraining COVID-19 transmission
- Cellular infectivity experiment results indicated that higher temperature decreased the half-life of SARS-CoV-2
- We provided integrated information to confirm the independent inhibiting effect of temperature on COVID-19 transmission

Contribution of Temperature Increase to Restrain the Transmission of COVID-19

Mengyuan Ren,[1,2,11] Rongjuan Pei,[3,11] Bahabaike Jiangtulu,[1,2,11] Junxi Chen,[1,2,11] Tao Xue,[1,2] Guofeng Shen,[4] Xiaoru Yuan,[5] Kexin Li,[6] Changxin Lan,[1,2] Zhen Chen,[3] Xinwen Chen,[3] Yun Wang,[3] Xiaoqian Jia,[1,2] Zewu Li,[1,2] Audil Rashid,[7] Tippawan Prapamontol,[8] Xiuge Zhao,[9] Zhaomin Dong,[10] Yali Zhang,[1,2] Le Zhang,[1,2] Rongwei Ye,[1,2] Zhiwen Li,[1,2] Wuxiang Guan,[3,*] and Bin Wang[1,2,*]

[1]Institute of Reproductive and Child Health, Peking University/ Key Laboratory of Reproductive Health, National Health Commission of the People's Republic of China, Beijing 100191, P. R. China

[2]Department of Epidemiology and Biostatistics, School of Public Health, Peking University, Beijing 100191, P. R. China

[3]Wuhan Institute of Virology, Center for Biosafety Mega-Science, Chinese Academy of Sciences, Wuhan, Hubei, China

[4]College of Urban and Environmental Sciences, Peking University, Beijing 100871, P. R. China

[5]Key Laboratory of Machine Perception (Ministry of Education), and School of EECS, Peking University, Beijing, China

[6]Institute of Geographic Sciences and Natural Resources Research, CAS, Beijing 100101, P. R. China

[7]Faculty of Science, Botany Department, University of Gujrat, Hafiz Hayat Campus, Gujrat-50700, Pakistan

[8]Research Institute for Health Sciences, Chiang Mai University, Chiang Mai 50200, Thailand

[9]State Key Laboratory of Environmental Criteria and Risk Assessment, Chinese Research Academy of Environmental Sciences, Beijing 100012, P. R. China

[10]Beijing Advanced Innovation Center for Big Data-Based Precision Medicine, Beihang University, Beijing 100191, China

[11]These authors contributed equally

*Correspondence: binwangpku@foxmail.com (B.W.); guanwx@wh.iov.cn (W.G.)

Received: August 11, 2020; Accepted: December 12, 2020; Published Online: December 15, 2020; https://doi.org/10.1016/j.xinn.2020.100071

Citation: Ren M., Pei R., Jiangtulu B., et al. (2021). Contribution of Temperature Increase to Restrain the Transmission of COVID-19. The Innovation **2(1)**, 100071.

The COVID-19 outbreak has already become a global pandemic and containing this rapid worldwide transmission is of great challenge. The impacts of temperature and humidity on the COVID-19 transmission rate are still under discussion. Here, we elucidated these relationships by utilizing two unique scenarios, repeated measurement and natural experiment, using the COVID-19 cases reported from January 23 – February 21, 2020, in China. The modeling results revealed that higher temperature was most strongly associated with decreased COVID-19 transmission at a lag time of 8 days. Relative humidity (RH) appeared to have only a slight effect. These findings were verified by assessing SARS-CoV-2 infectivity under the relevant conditions of temperature (4°C–37°C) and RH (> 40%). We concluded that temperature increase made an important, but not determined, contribution to restrain the COVID-19 outbreak in China. It suggests that the emphasis of other effective controlling polices should be strictly implemented to restrain COVID-19 transmission in cold seasons.

INTRODUCTION

Global transmission of coronavirus disease 2019 (COVID-19) caused by severe acute respiratory syndrome coronavirus-2 (SARS-CoV-2) is occurring on an unprecedented scale. The spread of confirmed cases has been sufficiently substantial that the event has already been declared a pandemic event. Controlling this rapid worldwide transmission is an imminent challenge. SARS-CoV-2 has gene sequences identical to those of SARS-CoV with more than 79.6% similarity.[1] In addition, its environmental stability is similar to that of the two other β-coronaviruses of SARS-CoV and MERS-CoV. For example, the half-lives of SARS-CoV-2 in aerosols and on surfaces of various materials are generally comparable with those of SARS-CoV.[2] Low temperature and low humidity favor the survival of both SARS-CoV and MERS-CoV.[3,4] Sajadi et al.[5] depicted a pattern of significantly high community transmission in countries coincidentally located in similar latitudes in the Northern Hemisphere (e.g., China, Iran, France, Italy, and the USA), which is linked with certain ranges of temperature (3°C–17°C) and absolute humidity (4–9 g/m^3).[6] Until now, the implication of COVID-19 transmission in view of fluctuating temperature and humidity is somewhat uncertain, but pertinent scientific questions need to be answered, not only for scientists but also, and more importantly, for the public and policymakers.

An experimental study indicated that the SARS-CoV-2 virus has multifactorial immune responses similar to those of the avian H7N9 disease.[7] It is well established that the transmission trend of influenza viruses (e.g., H1N1 and H7N9) depends greatly on the season.[8] However, until now, very little solid information has been available about the effects of temperature and humidity on the transmission rate of SARS-CoV-2, and this is also true for the previous SARS-CoV and MERS-CoV coronaviruses. We are aware of several studies on the association of temperature or humidity with the modulation of COVID-19 transmission in peer-reviewed journals or preprint websites of MedRxiv, BioRxiv, and SSRN. Most of them showed that increase in temperature or humidity may reduce transmission rates of COVID-19 on both regional and global scales.[9–14] Some other studies may have found the opposite phenomenon. For example, it has been reported that there was no dependence of the rate of spread of the COVID-19 pandemic on temperature.[15] Oliveiros et al.[16] pointed out that the transmission rate correlates positively with relative humidity. However, the latter claim is not consistent with the overall distribution characteristics of COVID-19,[6,17] nor previous environmental stability test results on SARS-CoV and MERS-CoV.[3,4] Soon after the Wuhan lockdown on January 23, 2020, localized COVID-19 cases, with minimal chances of intrusion from other areas, were examined by Luo et al.[18]; however, some other important potential confounders, especially those pertaining to heterogeneities among cities in China or around the world (e.g., availability of medical treatment in various cities, population mobility), incubation period, and meteorological differences between indoor and outdoor environments, were not well controlled. The same limitations also exist in the other aforementioned studies.[6,9–17,19] Provisioning of concrete evidence is therefore imperative. Based on current knowledge of the transmission characteristics of SARS-CoV-2, we proposed a hypothesis that both temperature and relative humidity can modulate the spread of COVID-19. To evaluate the causal effects of temperature and humidity on COVID-19 transmission, it is crucial to select an appropriate scenario in which important confounders can be controlled, and validate the relevant results with certain intervention evidence.

RESULTS AND DISCUSSION

We explored the relationships between the COVID-19 transmission rate and the relevant meteorological factors using the following four steps. First, we developed the relationship between daily cumulative increase of COVID-19 cases and time. After excluding cluster infection events (such as a cluster

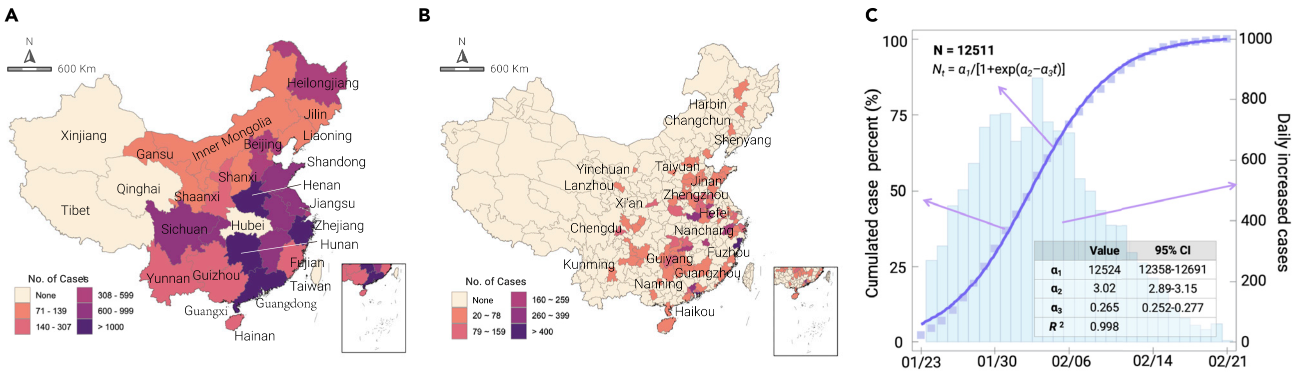

Figure 1. Cummulated Confirmed Cases of COVID-19 and Its Geographic Distribution The geographic distribution of the total confirmed COVID-19 cases in the 27 provinces (A) and 99 cities (B) included from January 23 to February 21, 2020; only the large typical cities were marked for readers' convenience. (C) The increasing trend of total COVID-19 cases from the 27 provinces. Cumulated confirmed case percent during that period is shown as scatters and fitting curve, corresponding to the left Y-axis. Daily increased cases are shown as vertical bars, corresponding to the right Y-axis. Total confirmed cases (N) of the 27 provinces as of February 21 was 12,511. The parameters of the fitted curve are shown in the table inserted in (C).

infection occurring in a prison) (Table S1), we found a tangible increase in the daily cumulative cases following a three-parameter logistic model for all geographic units under consideration for the selected 27 provinces and 99 cities (Table S2), the geographical information of which is provided in Figures 1A and 1B. For the 27 provinces, the increasing trends of cumulative COVID-19 cases with time were fitted by Equation (1) with high $R^2 > 0.97$ (see Figure S1). Here, we only show the increasing trend of the total COVID-19 cases from the 27 provinces, which could be fitted well with $R^2 = 0.998$ (see Figure 1C).

Second, we explored the associations of environmental temperature and relative humidity with transmission rate. The mean (minimum–maximum) ambient temperature and relative humidity in selected regions were 3.85°C (−27.17°C–24.47°C) and 79.66% (27.25%–100%) during the relevant period. The linear mixed model results showed that the transmission rate had an apparent association with temperature or relative humidity, which varied with the lag time (denoted LT), with a U-shaped relationship (Figure 2). At either the province or city level (Figures 2A and 2B), an overall broadly negative association was recorded between outdoor temperature and transmission rate when LT $\geq$ 5 days, and the above association (i.e., the absolute value of regression coefficients of β_1) was observed to be strongest when LT = 8 days, as highlighted by the gray rectangle. For relative humidity at the city level, a negative association with transmission rate was found when LT $\geq$ 8 days. At the province level, however, a statistically significant association between these was observed only when LT = 8 days (Figure 2C), which was not consistent with the results at the city level (Figure 2D). The sensitive analyses results (Figures S5 and S6) indicated that the above associations were overall consistent when mobility index was excluded from the model, or the event-based information was not corrected according to Table S1. We also confirmed the sensitivity of β_1 to the confounders of wind speed, precipitation, population mobility indexes, and population density (Figure S7). It seemed that the precipitation and mobility indexes had obvious effects on β_1, while the population density and wind speed had negligible effects. However, the overall results were consistent under the condition of excluding any of them. We further analyzed the interactive effects between temperature and relative humidity on the transmission rate of COVID-19 (see Table S3). No such effects were observed between them at either the province or city level, nor were effects observed with or without public central heating. It seemed that relative humidity did not have any modifying effects with temperature on the transmission rate. Therefore, the effect of relative humidity on the transmission rate is not analyzed in the following.

Shi et al.[20] reported that a lag period of meteorological conditions on COVID-19 transmission may exist among the population, which included the entire time from case infection with SARS-CoV-2 to the day when the infection confirmation information was reported on the official website. Using the distributions of incubation time[21] and report interval,[22] the estimated LT value was 10.0 (interquantile range: 6.3–14.8) days (Figure S8). For incubation time, another study reported a median incubation period, from as many as 1,099 confirmed cases, of 3 days,[23] which was about 2 days less than the median incubation time of 5.1 days used in our study.[21] In addition, the report interval was estimated based on national data, i.e., including Hubei Province, China,[22] which should be larger than those of other provinces because Hubei Province had limited medical resources during the period of rapid increase after January 23, 2020. Thus, the practical LT value of the other regions, except for Hubei Province, in China should have been smaller than the 10-day interval estimated from these data. Our modeling results revealed that the most probable LT value was 7 or 8 days, which was reasonable when considering the time estimate based on published studies.

With regard to temperature, we found that there seemed to be a strong inhibitory effect on the transmission rate of COVID-19, which is consistent with the results of studies published in peer-reviewed or posted on preprint websites.[6,9–14,16–19,24] Regarding relative humidity, a significant protective effect on COVID-19 transmission at the province level was found only when LT = 8 days, whereas a significant inhibiting effect at the city level was observed when LT = 8–13 days. Therefore, the effect of relative humidity does not appear to be stable like that of temperature, but it may account for a trivial inhibitory effect on the spread of COVID-19 based on our current data analysis. Moreover, the above-mentioned studies did not consider the lag period of environmental factors on the transmission rate. The lag time is the crucial parameter to link the meteorological conditions to the spreading rate of COVID-19 because there is a latent period between SARS-COV-2 infection and syndrome onset.

When LT = 8, we did not find any interactive effect between temperature and humidity on transmission rate. It had been proposed that the optimal temperature and relative humidity for COVID-19 transmission may be less than 5°C–11°C and 47%–79%, respectively.[17] In our study, more than half of the areas screened during the study period had a high relative humidity of more than 80% (Figures S2 and S3). Our study indicated that there was very slight inhibitory effect of relative humidity on transmission rate. Further studies need to be conducted to assess the effect of the coming monsoon in some Asian regions. In the sensitivity analyses, we found the confounders of precipitation and population mobility, but not population density or wind speed, had a significant effect on the value of β_1, which was not consistent with the study of Islam et al.[24] One possible explanation is that the virus shed by COVID-19 cases can be removed by rain. In addition, outdoor activities should decrease during rainy weather, resulting in a diminished chance of population infection by contacts.

Third, we also chose a natural experiment scenario to verify the effect of temperature. It has been reported that the population of China overall spends 83% of time indoors.[25] Therefore, the outdoor temperature cannot represent

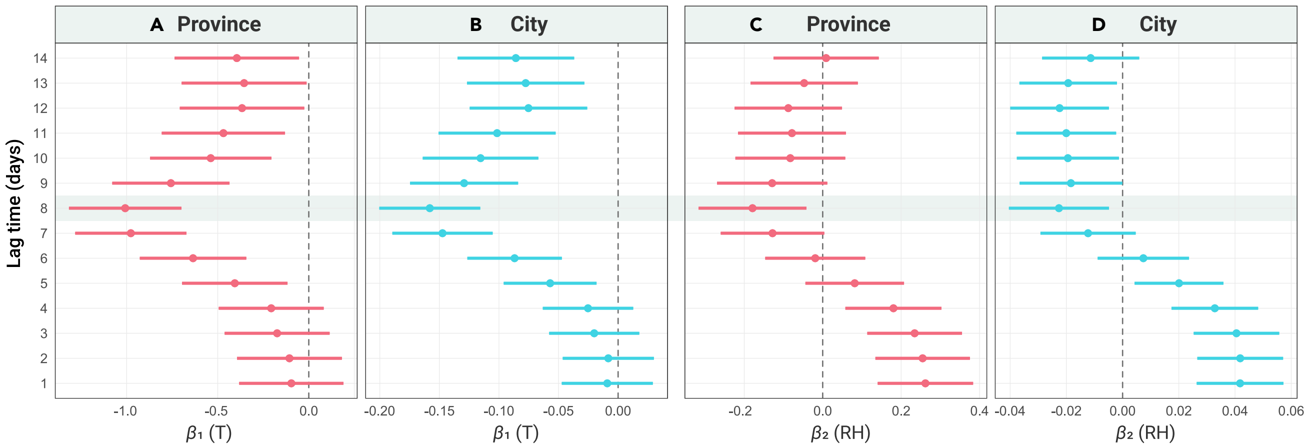

Figure 2. Ambient Temperature & Relative Humidity and COVID-19 Transmission Associations of ambient temperature (A, province level; B, city level) and relative humidity (C, province level; D, city level) with the transmission rate of COVID-19. Transmission rate was defined as the increased rate of cumulated confirmed cases per day in a logistic growth model: Equation (1). The regression coefficients (β_1 and β_2) were obtained using a linear mixed-effect model as follows: $R_{[t,\ s]} = \beta_1 T_t + \beta_2 RH_t + \beta_3 WS_t + \beta_4 PR_t + \beta_5 MII_t + \beta_6 MOI_t + \beta_7 PD_t + \gamma(L)$. This formula incorporated seven fixed terms ($\beta_{1\text{-}7}$) to model the effects of temperature (*T*), relative humility (*RH*), wind speed (*WS*), precipitation (*PR*), population mobility indexes of moving-in (*MII*) and moving-out (*MOI*), population density (*PD*), and a random intercept (γ) to control for the location (*L*)-specific effects. Data are shown with an estimated value with 95% confidence interval.

the real ambient environmental living conditions for those with public central heating. If an effect of a meteorological variable on transmission rate existed, the maintenance of different household temperatures could strengthen or weaken the association, which can be verified by adding an interaction term of temperature or relative humidity with public central heating status. Here, a significant modification effect of public central heating status on the association between temperature and transmission rate ($p < 0.05$) was observed when LT = 5–10 days (Figure 3A). For areas without public central heating, the decrease of transmission rate seemed larger than for areas with public central heating at both the province and city levels. The most obvious coefficient (β_1) was also found when LT = 7 or 8 days. These associations were consistent overall without adjusting the mobility indexes (Figure S9). Here, two views can be promulgated. The first is that the outdoor temperature is less likely to be consistent with the actual living conditions of the population residing in northern China, which might have caused a relatively low transmission rate depending on the outdoor temperature in northern China compared with that in southern China. The second view highlights the nature of the heating facilities, which is public central heating and shared among populations confined within geographic units, with limited mobility, thus creating a condition that may trigger further changes in transmission rate. Nevertheless, this natural experiment scenario, which was not documented in previously reported studies, is highly relevant to validation of our findings related to temperature effects. This suggests a decisive role of temperature control as an efficient phenomenon in the regulation of COVID-19 transmission rate in residential environments over large areas. We subsequently compared the variance of β_1 among the relevant provinces and cities (Figure 3B), and the detailed data are provided in Table S4. Overall, higher magnitudes of change of transmission rate with temperature were found in the provinces or cities in southern China (e.g., the top five provinces were Henan, Anhui, Hunan, Jiangxi, and Guangdong) than in those in northern China (e.g., the last five were Liaoning, Jilin, Inner Mongolia, Shanxi, and Hebei). The nonlinear relationship between ambient temperature and COVID-19 transmission is shown in Figure S10 when LT = 8 days. It seemed that their relationship was close to being linear, but a temperature threshold was not found. When assuming that T_{ref} was the 1-week average temperature around the date of LT earlier than January 23, 2020, the dependence of the reduction in COVID-19 cases with LT (ΔN_M) was estimated taking into consideration of the geographic variance of the effect of temperature on the transmission rate. During the relevant period, we estimated that there were about 4,066 persons who were not affected by SARS-CoV-2 due to the temperature increase when LT = 8 days. The detailed results of ΔN_M of other lag times are shown in Table S5. In this natural experiment scenario, the distribution of central heating is not randomly distributed in China, i.e., only some northern provinces with very low temperature during the winter season have municipally supplied central heating, while the southern provinces do not. This allows us to conduct the stratification analysis by using the public central heating status.

Fourth, we utilized virus persistence experiments to test the effects of temperature and relative humidity on SARS-CoV-2 infectivity. The residual viral infectivity was titrated at different time points (Figure 4A). We found that the titer decrease mainly occurred in the first 4 h after the first-order decay trend, of which the half times were calculated (Figure 4B). The detailed viral titer at each time point is given in Table S6. There was a decreasing trend of half-time with incubation temperature (ANOVA test $p < 0.05$), especially under high humidity conditions. Pairwise comparison results also indicated that significant differences were observed at 20°C versus 28°C under low relative humidity conditions, 4°C versus 37°C and 20°C versus 37°C under high relative humidity condition (Tukey adjusted $p < 0.05$), respectively. At 4°C, SARS-CoV-2 maintained a high residual titer, even up to 72 h, with ~4 Log_{10}PFU/mL. The reduction was more dramatic when the temperature exceeded 28°C and almost no live virus could be observed after 24 h incubation (Figure 4A). Under both low and high relative humidity conditions, the trends of residual titers (Log_{10}PFU/mL) of SARS-CoV-2 were similar. For the half times during the first 4 h, we only observed a significant difference between high and low relative humidity at 20°C (Tukey's adjusted $p < 0.05$).

The laboratory experimental study provides a more ideal scenario by controlling other confounders. While the modeling study, conducted based on the daily confirmed cases and meteorological data, reflects an uncontrolled but real-life situation. Although it is difficult to harmonize the related findings from these two approaches, they both can contribute to explain the effects of temperature and humidity on the transmission rate of SARS-CoV-2.[26] Previous studies showed that the infectivity of SARS-CoV significantly decreased with increase in temperature from 28°C to 38°C and decreased more rapidly from 35°C to 38°C.[3] MERS-CoV was shown to be more stable at low temperature/low humidity conditions. Our results, implying that the coronavirus is more stable at lower temperatures, especially at 4°C, were consistent with previous results. However, relative humidity plays different roles with regard to these viruses. A strong inhibitory effect of humidity on infectivity of SARS-CoV was found mainly when the temperature was >28°C.[3] MERS-CoV was more stable at low humidity conditions, but no relative humidity effect on stability was observed for SARS-CoV-2. However, in a previous study, only three experimental conditions of temperature and relative humidity (i.e., 20°C and 40%, 30°C and 30%, and 30°C and 80%) were chosen, and these could not facilitate analysis of any independent effect of temperature or relative

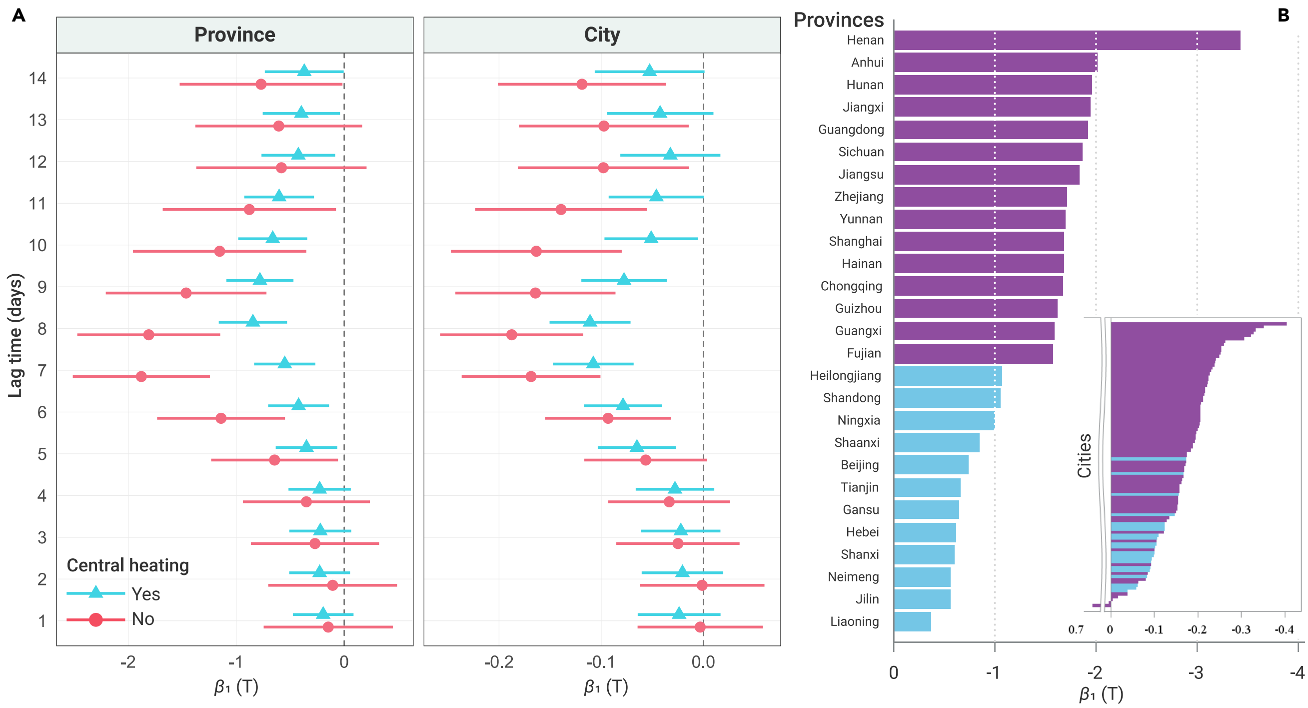

Figure 3. Modification Effect of the Central Heating Status Modification effect of the central heating status on the association of ambient temperature with the transmission rate of COVID-19 (A) and geographic variances of the effects of temperature on the transmission rate when LT = 8 days (B). Transmission rate was defined as the increased rate of cumulated confirmed cases per day in a logistic growth model: Equation (1). The regression coefficient (β_1) was obtained using a linear mixed-effect model as follows: $R_{[t,\,s]} = \beta_1 T_t + \beta_2 RH_t + \beta_3 WS_t + \beta_4 PR_t + \beta_5 MII_t + \beta_6 MOI_t + \beta_7 PD_t + \gamma(L)$. This formula incorporated seven fixed terms ($\beta_{1\text{-}7}$) to model the effects of temperature (*T*), relative humility (*RH*), wind speed (*WS*), precipitation (*PR*), population mobility indexes of moving-in (*MII*) and moving-out (*MOI*), population density (*PD*), and a random intercept (γ) to control for the location (*L*)-specific effects. For (A), the data are shown with an estimated value with a 95% confidence interval. For (B), the geographic areas with central heating are indicated in blue and those without in purple.

humidity.[4] Our study included relatively more exposure conditions of temperature by referring to the ambient environments in the study regions during the study period. To our surprise, SARS-CoV-2 could maintain high infectivity at 4°C even after 72 h (3 days). However, the residual infectivity decreased dramatically when the temperature exceeded 20°C. Another study investigated the stability of SARS-CoV-2 on cloth at room temperature (22°C) and a relative humidity (~65%) with the initial titer (4.84 Log_{10}TCID50/mL), which was comparable with one of the conditions in our study where the room temperature was 20°C and relative humidity was around 40%–60% with an initial titer of 4.56 Log_{10}PFU/mL. Overall, the decay rate in our study was relatively lower than that on cloth,[27] but it cannot be well explained using the current data. The choice of the materials may cause different results between studies, which needs confirmation in further studies. Compared with temperature, relative humidity seemed to have a weak effect on the stability of SARS-CoV-2. In a previous infectivity study, it was reported that the viability of SARS-CoV-2 significantly decreased with increase of relative humidity from 20% to 60%, but not from 60% to 80%.[28] Our study further showed the dependence of SARS-CoV-2 infectivity on relative humidity from 40%–60% to 100%. Among the included cities, the relative humidity mostly ranged from 60% to 95%. This can partly explain our modeling findings to a certain extent. However, one must be aware that social distancing between susceptible persons is important in addition to the change of virus stability. Our study provided very comprehensive experimental results pertaining to the stability of SARS-CoV-2 under ambient conditions of temperature and relative humidity.

Some previous studies have indicated nonlinear associations between respiratory infections (e.g., influenza) and the year-round temperature range.[29] However, because the COVID-19 epidemic was mostly well controlled in most regions of the Chinese Mainland, we cannot conduct a comparison study between the winter and summer seasons to provide more solid evidence. Our study only focused on our hypotheses at the limited range of meteorological conditions, which makes it difficult to extrapolate our results to more broad temperature ranges. The results obtained through our model were based on only a portion of the regions on Mainland China. Extrapolation of our results into areas with different geographical conditions should be done with care. Even within China, a stronger effect of temperature on COVID-19 transmission rate was observed in the southern regions. We did not take family-cluster infections into account, which might bias our results. We also did not consider the asymptomatic COVID-19 infection cases[32] due to limited data. Further studies are still needed to investigate the relationship between asymptomatic infection and transmission of COVID-19. Our virus persistence experiments only utilized gauze with suspended virus in working solution to investigate the relationship between SARS-CoV-2 infectivity and environmental temperature and humidity, which can only represent the real environment to a certain extent and the related results should be extrapolated with care. Nevertheless, the findings presented here have some advantages due to their demonstration of the effects of temperature and humidity on the transmission of COVID-19 in practical living scenarios in combination with the results of environmental stability for SARS-CoV-2. First, prevention and control policies in China can be executed simultaneously and forcefully in the province of concern. After January 23, 2020, there were only sporadic imported cases from Hubei Province in other cities. From the sensitivity analysis, we found that the model results were consistent with or without modification of imported and cluster infection cases. Second, the effects of temperature and humidity were investigated using a quasi-repeated measurement study followed by a linear mixed-effect model to control, to some extent, the differences among various regions in medical availability and executive force following the prevention and control plan issued by the National Health Commission (NHC) in China. Third, we adopted a natural experiment by using the public central heating status, which could significantly distinguish the intervention effect of temperature and humidity in the living environment. Fourth, the LT values, due to their lag effect on the transmission rate, were reasonably estimated at 7 or 8 days. It is crucial for us to

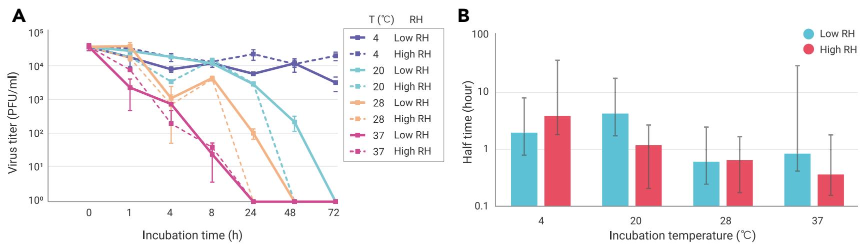

Figure 4. Environmental Persistence of SARS-CoV-2 The viability of SARS-CoV-2 under various temperature conditions (4°C, 20°C, 28°C, and 37°C) and relative humidity (RH) (low [L]: 40%–60%; high [H] > 99%) with time (0, 1, 4, 8, 24, and 48 h) on the surface of gauze cloth (A) and their half time of decay (B). The initial titer of the working virus solution was approximately 4.56 Log_{10}(PFU)/mL. (A) The experiments are conducted in replicates and the mean values and standard error of virus titer are shown. (B) The half-time was calculated according to the first 4-h virus viability and the 95% confidence interval was added as the error bar. The differences between the two groups were compared by Tukey's honestly significant difference pairwise comparison test.

estimate the relatively accurate effect of temperature on transmission rate. Finally, to the best of our knowledge, this is the first investigation to examine the effects of temperature and relative humidity on SARS-CoV-2 using a cellular experiment. Overall, the cellular infectivity results provided considerable supportive evidence for our modeling results.

Conclusions

Based on the results from the modeling and environmental stability analysis of SARS-CoV-2, we finally highlighted an emerging trend that increase in ambient temperature, irrespective of relative humidity, had a strong influence on restraining the transmission rate of COVID-19 in China. For the cold seasons, the emphasis on social distancing should be strictly implemented to restrain COVID-19 transmission. Still, we need other efficient prevention and control measures to entirely halt COVID-19 transmission.

MATERIALS AND METHOD

Information of Confirmed COVID-19 Cases

Numbers of daily confirmed cases for all of the Chinese cities or provinces of concern, during the period of January 23 to February 21, 2020, were collected from official reports on the website of the National Health Commission (NHC) or Provincial Health Commission (PHC) of China. Confirmed cases were defined as suspected cases with a positive test result for viral nucleic acid. In some cases, the Chinese NHC or PHC might have reported the "wrong" number of confirmed cases (but they made correction reports the following day); in such a situation, we would calculate "negative increase case number." Another situation existed when aggregation infection events occurred, the striking increase of which was obviously caused by close contact and confirmed by a rapid concentrated virus nucleic acid test. We denoted both situations as "abnormal data" (a detailed description is given in Table S1). A sensitivity analysis was conducted to compare the key findings with and without correction of the abnormal data. The data of daily increased COVID-19 cases, with and without corrections, are provided in Data S1. In addition, there were no imported cases from abroad.

Mobility Data, Population Density, Temperature, and Relative Humidity

A human mobility index from the Baidu Company was used to indicate individual movement among the provinces or cities of concern in our simulation study (see: http://qianxi.baidu.com/). The data were collected using the application program interface from the platform, and the information is given in Data S2. Population density was calculated by using 2017 census data in China at the county level. The daily averages of temperature and relative humidity were collected from the National Centers for Environmental Prediction (NCEP) reanalyzed climate database provided by the NOAA/OAR/ESRL PSD, Boulder, Colorado, USA. The data can be accessed freely from their website: https://www.esrl.noaa.gov/psd/. The product was based on a state-of-the-art data assimilation approach, which combined *in situ* observations with climate forecast results. We obtained the meteorological data in the two pixels that covered the city areas, and aggregated them into one daily time series for each variable. Their spatial resolution was 2.5° × 2.5°. The original data were obtained using the R package "RNCEP." The information included geographic distributions of average temperature and relative humidity (Figure S2), as well as the daily changes in temperature and relative humidity (Figure S3), at both the province and city levels. The information is included in Data S3.

Study Area and Duration

Since January 23, 2020, travel restrictions had been implemented for Wuhan. Intervention in the COVID-19 transmission rate of Hubei Province was exceptional because of the strong control policies; complex local situations also played a part. We therefore excluded regions of Hubei Province from this study. In total, 29 provinces or regions in Mainland China, as well as their 461 cities, were originally included in our model. For the geographic units of concern, we further excluded units with cumulative confirmed COVID-19 cases <20, and the fitting coefficient of determination (R^2) was $\leq$0.97. For example, the two provinces of Tibet and Qinghai were excluded due to their small numbers of COVID-19 cases. The fitting results are displayed in detail in Figure S1. During the second (announced on January 23, 2020) and fifth (announced on February 22, 2020) versions of the COVID-19 prevention and control plan from the Chinese NHC, the outbreak of COVID-19 in China had two main stages: a phase with rapid increase and a stationary phase. Moreover, during this period there seemed to be no obvious trend of warming, which may slightly bias our analyses results (See Figure S3). Therefore, we chose the period from January 23 to February 21, 2020, for data analysis. During this time, all of the provinces simultaneously implemented the NHC prevention and control plan with high executive force, as monitored by the central government inspection team.

Model Design

We first derived the daily infection transmission rate of COVID-19 for each geographic unit using a logistic growth model. The daily count of COVID-19 cases in each region ($N_{[t,\ s]}$) was assumed to increase with time (t), following a nonlinear curve, pre-determined by three parameters. The model can be specified as follows:

$$N_{[t,\ s]} = \alpha_1/[1 + \exp(\alpha_2 - \alpha_3 t)], \qquad \text{(Equation 1)}$$

where α_1, α_2, and α_3 are tuning parameters and can be estimated by finding the minimum of the residual sum of squares of the model. Therefore, the daily transmission rate ($R_{[t,\ s]}$) of COVID-19 at time t in region s is the first derivative of Equation (1), which can be calculated as follows:

$$R_{[t,\ s]} = \alpha_1/[1 + \exp(\alpha_2 - \alpha_3 t)]^2 \times \exp(\alpha_2 - \alpha_3 t) \times \alpha_3. \qquad \text{(Equation 2)}$$

Given differences in social distances, control policies, and many other aspects for each geographic unit, we fitted a logistic growth model and calculated a time series of daily transmission rate of [$R_1, R_2, \ldots, R_D$] for the duration of concern of D days in each region. The cumulative number of daily increased COVID-19 cases is equal to ΣN_t (noted as N). We then explored the relationship between the daily transmission rate and the independent variables of concern using a linear mixed-effect model, specified as follows:

$$R_{[t,\ s]} = \beta_1 T_t + \beta_2 RH_t + \beta_3 WS_t + \beta_4 PR_t + \beta_5 MII_t + \beta_6 MOI_t + \beta_7 PD_t + \gamma(L) \qquad \text{(Equation 3)}$$

The model incorporated seven fixed terms with coefficients of β_{1-7} to model the effects of the four meteorological factors of temperature (T), relative humidity (RH), wind speed (WS), and precipitation (PR), the two population mobility indexes (moving-in index [MII] and moving-out index [MOI]), and the population density (PD), as well as a random intercept to control for location (L)-specific effects (e.g., size of susceptible population, social distancing, medical resources, COVID-19 control policies), which were unavailable. Population migration between cities could also affect the daily transmission rates. Particularly, during the period surrounding the Chinese New Year ("Spring Festival") on January 25, 2020, between-city migration increased dramatically. Therefore, we incorporated the population mobility index of moving in or moving out (i.e., MII and MOI) as covariates in the model.

Effects of Temperature and Relative Humidity on the Stability of SARS-CoV-2

To illustrate the relationship between COVID-19 transmission and meteorological factors, we further utilized a virus persistence experiment. SARS-CoV-2 was isolated from the bronchoalveolar lavage fluid of a patient[1] and passaged in a monkey kidney cell line (Vero-E6) for eight generations. The titer of the SARS-CoV-2 working solution was ~5 × 10^5 plaque-forming units (PFU)/mL, as determined by plaque assay on the Vero-E6 cells incubated in the culture medium (DMEM with 2% FBS). Ninety-six cotton gauzes were prepared for the exposure experiment and placed in culture dishes, which were placed in incubators without light. A volume of 50 μL of SARS-CoV-2 working solution in DMEM culture medium with 2% FBS was spotted in droplets on the cotton gauze, dried for 30 min in a biological safety cabinet, and then incubated under specific temperature conditions (4°C, 20°C, 28°C, and 37°C) and relative humidity (low and high). In this stage, there was an immediate reduction in infectivity of the virus during drying in culture medium. After 30 min drying, they were incubated for about 1, 4, 8, 24, 48, and 72 h, respectively. At each exposure time point, the cotton gauzes were collected and soaked in 400 μL DMEM for 10 min, and the infectivity of the lixivium was then determined by plaque assay. For the high humidity groups, papers soaked with ultrapure water were placed in a zip-lock bag with the culture dish and cotton gauze inside. However, we could not measure the relative humidity directly. To mimic this environment, the wet paper tower was placed in a sealed box of an appropriate size, and the relative humidity was measured to be higher than 99% within 1 h measured using a psychrometer (Deli, model 9026, Ningbo City, China). Therefore, the relative humidity in the sealed bags with the wet paper towel was expected to be higher than 99%. The experiment was conducted in an animal biosafety level-III lab, where the indoor relative humidity was kept consistently at 40%–60%; this was measured using the same psychrometer and adopted as the low relative humidity in our study. The relative humidity in the bags without the wet paper towel was expected to be the same as the indoor relative humidity in the room. All experiments were conducted in replicates.

Data Analysis

The logistic growth model was executed using SAS software (SAS University Edition). The nonlinear (NLIN) regression procedure was used where the Gauss-Newton algorithm was utilized to search for the parameters that produced the smallest residual sum of squares. At the same time, the transmission rate was subsequently calculated based on Equation (2). Calculation of the linear mixed-effect model and mapping of the geographic distribution of the data of concern were carried out using the R package of "lme4" using R software (version 3.6.1). Cities were dynamically included if they were simultaneously accompanied by information on temperature, humidity, wind speed, precipitation, mobility, and population density at the lag times of concern with an assumed range of 1–14 days. Considering that the absolute humidity is highly positively correlated with the temperature ($r = 0.938$, $p < 0.001$) (see Figure S4A), it is not appropriate to adopt them together in our linear model due to the multicollinearity. Theoretically, the absolute humidity is significantly influenced by the environmental temperature. Likewise, temperature has been proved to be an independent factor that affects virus stability, thus we chose only the temperature, rather than the absolute humidity, as the main independent variable. The relative humidity is also statistically correlated with temperature (see Figure S4B), but has a very weak correlation ($r = 0.27$, $p < 0.001$), resulting in a negligible effect on the linear regression model. In considering that we had integrated information of temperature, absolute humidity, and atmospheric pressure, we therefore adopted this in our mixed model analysis. To validate the robustness of our model results, we further conducted sensitivity analyses by excluding the mobility index, or without correction by the event-based information. We also further confirmed the sensitivity of β_1 to the confounders of wind speed, precipitation, population mobility indexes, and population density.

For data interpretation, we adopted the "lag time" (LT) to evaluate the environmental lag period of temperature or relative humidity, i.e., the period from the case infection of SARS-CoV-2 to the day when infection confirmation information was reported on the NHC website. This time period included the two main intervals of the time between the person being infected by SARS-CoV-2 and the onset of symptoms (i.e., the incubation time) and the time between the onset of symptoms and the report after infection confirmation on the NHC website (i.e., the report interval). These two intervals both followed gamma distributions, and their parameters were both provided in previous studies.[21,22] The value distribution of LT was obtained by summing incubation time and report interval, which was carried out using SAS software. Subsequently, the LT value was used to compare our modeling results.

To further examine the association between temperature and relative humidity on COVID-19 transmission rate, we explored whether the linkage was modified by maintained household temperature. After January 23, 2020, most residents were encouraged to minimize their outdoor activities, and household heating considerably affected the indoor environment. In China, almost all household heating is municipally supplied at the city level, denoted as "public central heating," and this is determined by geographical latitude in China. The Ministry of Housing and Urban-Rural Development of the People's Republic of China requires that the critical outdoor temperature for municipal heating is 5°C.[30] On the other hand, the China District Heating Association requires that the municipally supplied indoor heating temperature should not be lower than 18°C.[31] Therefore, in cities with public central heating, the indoor-versus-outdoor differences in temperature and relative humidity were obviously larger than those in cities without public central heating. If an effect of a weather variable on COVID-19 transmission existed, different household temperature control could strengthen or weaken the association. To check the above hypothesis, we incorporated the public central heating status of each city as an effect modifier and modeled its interactions with both temperature and relative humidity.

To investigate the nonlinear relationship of ambient temperature on COVID-19 transmission at the longest possible lag time, a generalized additive mixed model with random intercept was utilized using the R package of "mgcv."

We constructed a scenario by assuming that the average of the relevant meteorological factors among the relevant geographic areas remains unchanged during the study period after the date of the earlier lag time before the January 23, 2020, around which the average meteorological condition was set as the reference (M_{ref}). The daily change of R_t (ΔR_t) can be obtained by the product of β_M ($M_t - M_{ref}$), where β_M is the regression coefficient of the relevant meteorological factor from Equation (3). Thus, the accumulated number of COVID-19 cases (ΔN_M) associated with the change of the individual relevant meteorological factor during the D days is equal to $\Sigma\beta_M$ ($M_t - M_{ref}$).

For the results of the virus persistence experiments, we calculated the half times by assuming that they followed first-order decay. An ANOVA test was used to compare the mean difference of half times among different temperature and humidity treatments. Tukey's honestly significant difference pairwise comparison was also performed to compare the differences among all possible combination of treatments, and Tukey's adjusted p value was used to indicate the false-positive statistical results. The key analysis code is provided in the Supplemental Code file.

REFERENCES

1. Zhou, P., Yang, X.L., Wang, X.G., et al. (2020). A pneumonia outbreak associated with a new coronavirus of probable bat origin. Nature ***579***, 270–273.
2. van Doremalen, N., Bushmaker, T., Morris, D.H., et al. (2020). Aerosol and surface stability of SARS-CoV-2 as compared with SARS-CoV-1. N. Engl. J. Med. https://doi.org/10.1056/NEJMc2004973.
3. Chan, K.H., Peiris, J.S., Lam, S.Y., et al. (2011). The effects of temperature and relative humidity on the viability of the SARS coronavirus. Adv. Virol. ***2011***, 734690.
4. van Doremalen, N., Bushmaker, T., and Munster, V.J. (2013). Stability of Middle East respiratory syndrome coronavirus (MERS-CoV) under different environmental conditions. Euro Surveill. ***18***, https://doi.org/10.2807/1560-7917.es2013.18.38.20590.
5. Sajadi, M.M., Habibzadeh, P., Vintzileos, A., et al. (2020). Temperature, humidity, and latitude analysis to estimate potential spread and seasonality of coronavirus disease 2019 (COVID-19). JAMA Netw. Open ***3***, e2011834.
6. Bukhari, Q., and Jameel, Y. (2020). Will coronavirus pandemic diminish by summer? SSRN. . [preprint]. https://doi.org/10.2139/ssrn.3556998.
7. Thevarajan, I., Nguyen, T.H.O., Koutsakos, M., et al. (2020). Breadth of concomitant immune responses prior to patient recovery: a case report of non-severe COVID-19. Nat. Med. https://doi.org/10.1038/s41591-020-0819-2.
8. Paules, C., and Subbarao, K. (2017). Influenza. Lancet ***390***, 697–708.
9. Ma, Y., Zhao, Y., Liu, J., et al. (2020). Effects of temperature variation and humidity on the death of COVID-19 in Wuhan, China. Sci. Total Environ. ***724***, 138226.
10. Zhu, L., Liu, X., Huang, H., et al. (2020). Meteorological impact on the COVID-19 pandemic: a study across eight severely affected regions in South America. Sci. Total Environ. ***744***, 140881.
11. Wu, Y., Jing, W., Liu, J., et al. (2020). Effects of temperature and humidity on the daily new cases and new deaths of COVID-19 in 166 countries. Sci. Total Environ. ***729***, 139051.
12. Demongeot, J., Flet-Berliac, Y., and Seligmann, H. (2020). Temperature decreases spread parameters of the new Covid-19 case dynamics. Biology (Basel) ***9***, https://doi.org/10.3390/biology9050094.
13. Qi, H., Xiao, S., Shi, R., et al. (2020). COVID-19 transmission in Mainland China is associated with temperature and humidity: a time-series analysis. Sci. Total Environ. ***728***, 138778.
14. Shi, P., Dong, Y., Yan, H., et al. (2020). Impact of temperature on the dynamics of the COVID-19 outbreak in China. Sci. Total Environ. ***728***, 138890.
15. Yao, Y., Pan, J., Liu, Z., et al. (2020). No association of COVID-19 transmission with temperature or UV radiation in Chinese cities. Eur. Respir. J. ***55***, https://doi.org/10.1183/13993003.00517-2020.
16. Oliveiros, B., Caramelo, L., Ferreira, N.C., et al. (2020). Role of temperature and humidity in the modulation of the doubling time of COVID-19 cases. medRxiv. . [preprint]. https://doi.org/10.1101/2020.03.05.20031872.
17. Sajadi, M.M., Habibzadeh, P., Vintzileos, A., et al. (2020). Temperature and latitude analysis to predict potential spread and seasonality for COVID-19. SSRN. . [preprint]. https://doi.org/10.2139/ssrn.3550308.
18. Luo, W., Majumder, M.S., Liu, D., et al. (2020). The role of absolute humidity on transmission rates of the COVID-19 outbreak. medRxiv. . [preprint]. https://doi.org/10.1101/2020.02.12.20022467.
19. Wang, M., Jiang, A., Gong, L., et al. (2020). Temperature significantly change COVID-19 transmission in 429 cities. medRxiv. . [preprint]. https://doi.org/10.1101/2020.02.22.20025791.
20. Shi, P., Dong, Y., Yan, H., et al. (2020). The impact of temperature and absolute humidity on the coronavirus disease 2019 (COVID-19) outbreak—evidence from China. medRxiv. . [preprint]. https://doi.org/10.1101/2020.03.22.20038919.
21. Lauer, S.A., Grantz, K.H., Bi, Q., et al. (2020). The incubation period of coronavirus disease 2019 (COVID-19) from publicly reported confirmed cases: estimation and application. Ann. Intern. Med. ***172***, 577–582.

22. Li, R., Pei, S., Chen, B., et al. (2020). Substantial undocumented infection facilitates the rapid dissemination of novel coronavirus (SARS-CoV-2). Science ***368***, 489–493.
23. Guan, W.J., Ni, Z.Y., Hu, Y., et al. (2020). Clinical characteristics of coronavirus disease 2019 in China. N. Engl. J. Med. ***382***, 1708–1720.
24. Islam, N., Shabnam, S., and Erzurumluoglu, A.M. (2020). Temperature, humidity, and wind speed are associated with lower Covid-19 incidence. medRxiv. . [preprint]. https://doi.org/10.1101/2020.03.27.20045658.
25. Wang, B., Wang, Z., Zhao, X., et al. (2014). Investigation on indoor and outdoor time of Chinese adults. J. Environ. Health ***31***, 945–948, [in Chinese].
26. National Academies of Sciences, E. (2020). Medicine, Rapid Expert Consultation on SARS-CoV-2 Survival in Relation to Temperature and Humidity and Potential for Seasonality for the COVID-19 Pandemic (April 7, 2020) (The National Academies Press), p. 8.
27. Chin, A.W.H., Chu, J.T.S., Perera, M.R.A., et al. (2020). Stability of SARS-CoV-2 in different environmental conditions. Lancet Microbe ***1***, e10.
28. Biryukov, J., Boydston, J.A., Dunning, R.A., et al. (2020). Increasing temperature and relative humidity accelerates inactivation of SARS-CoV-2 on surfaces. mSphere ***5***, https://doi.org/10.1128/mSphere.00441-20.
29. Dai, Q., Ma, W., Huang, H., et al. (2018). The effect of ambient temperature on the activity of influenza and influenza like illness in Jiangsu Province, China. Sci. Total Environ. ***645***, 684–691.
30. MOHURD, Design Code for Heating Ventilation and Air Conditioning of Civil Buildings. 2012,
31. CDHA (2020). Urban Heating service. http://www.china-heating.org.cn/hangyebz/471710200.html.
32. Jia, Xiaoqian, Chen, Junxi, Li, Liangjing, et al. (2020). Modeling the Prevalence of Asymptomatic COVID-19 Infections in the Chinese Mainland. The Innovation ***1***, 100026.

ACKNOWLEDGMENTS

We would like to express our gratitude for discussions with the researchers from the environmental exposure and human health working group of the China Cohort Consortium (http://chinacohort.bjmu.edu.cn/), as well as special thanks to Dr. Ping Zhong and Dr. Wentao Wang for their instructive guidance. This work was supported by the National Key Research and Development Program, P.R. China (Grant No. 2020YFC0846300 and 2020YFC0846200) and the National Natural Science Foundation of China (Grant No. 41771527; 41922057).

AUTHOR CONTRIBUTIONS

B.W., M.R., B.J., J.C., T.X., G.S., and X.Y. conceived the study. B.J., J.C., and T.X. curated the data. M.R., B.J., J.C., and T.X. performed the analysis. B.W., T.X., M.R., and K.L. wrote the first draft of the manuscript. R.P., Z.C., X.C., F.D., and W.G. finished the virus stability experiment. R.P., C.L., Z.C., X.C., F.D., X.J., L.Z., R.Y., Z.D., K.L., L.Z., Y.Z., G.Z., and W.G. reviewed and edited the manuscript. B.W. and Z.L. managed the program.

DECLARATION OF INTERESTS

All authors declare no competing interests.

SUPPLEMENTAL INFORMATION

Supplemental Information can be found online at https://doi.org/10.1016/j.xinn.2020.100071.

The Innovation, Volume *2*

Supplemental Information

Contribution of Temperature Increase

to Restrain the Transmission of COVID-19

Mengyuan Ren, Rongjuan Pei, Bahabaike Jiangtulu, Junxi Chen, Tao Xue, Guofeng Shen, Xiaoru Yuan, Kexin Li, Changxin Lan, Zhen Chen, Xinwen Chen, Yun Wang, Xiaoqian Jia, Zewu Li, Audil Rashid, Tippawan Prapamontol, Xiuge Zhao, Zhaomin Dong, Yali Zhang, Le Zhang, Rongwei Ye, Zhiwen Li, Wuxiang Guan, and Bin Wang

Supplemental Materials

This file includes:

Figs. S1 to S10

Tables S1, S3 to S6 (Table S2 is provided as another individual excel file.)

Other Supplemental Materials for this manuscript include the following:

Table S2: The increasing trend of the confirmed COVID-19 cases during Jan. 23–Feb. 21, 2020 and their fitting parameters using a Logistic model for the selected 27 provinces and 99 cities.

Data S1: The data of daily increased COVID-19 cases with and without corrections from the NHC website report.

Data S2: Human mobility index used to indicate of the individual movement among the concerned provinces or cities in our study. Sourced from the Baidu Co. service (see the website: http://qianxi.baidu.com/.

Data S3: The temperature and relative humidity during the study period in our study.

Supplementary Code: The analysis R code for the key calculations.

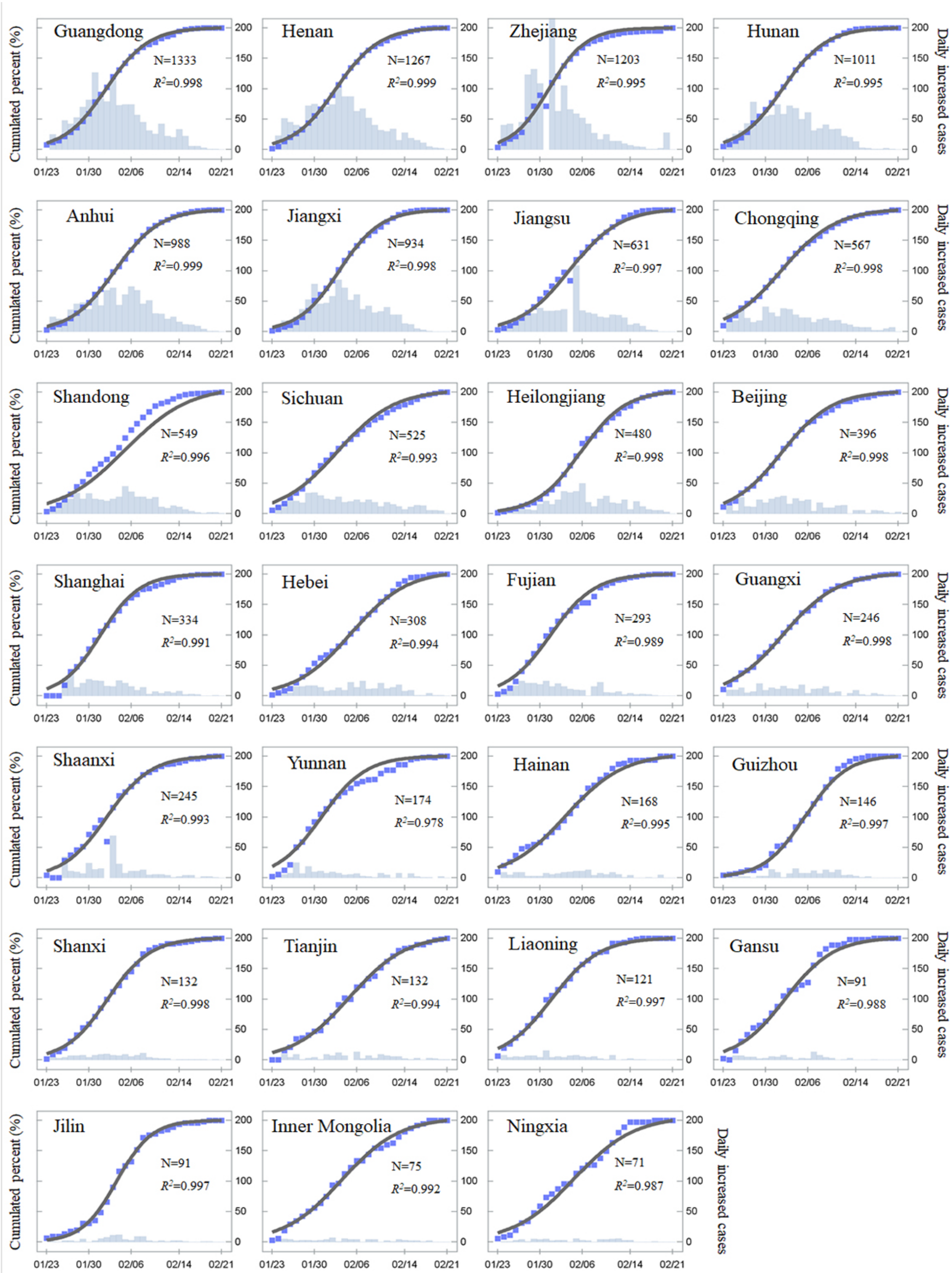

Figure S1. The fitting curve of the increase trend of the COVID-19 cases in the individual 27 provinces of Chinese Mainland.

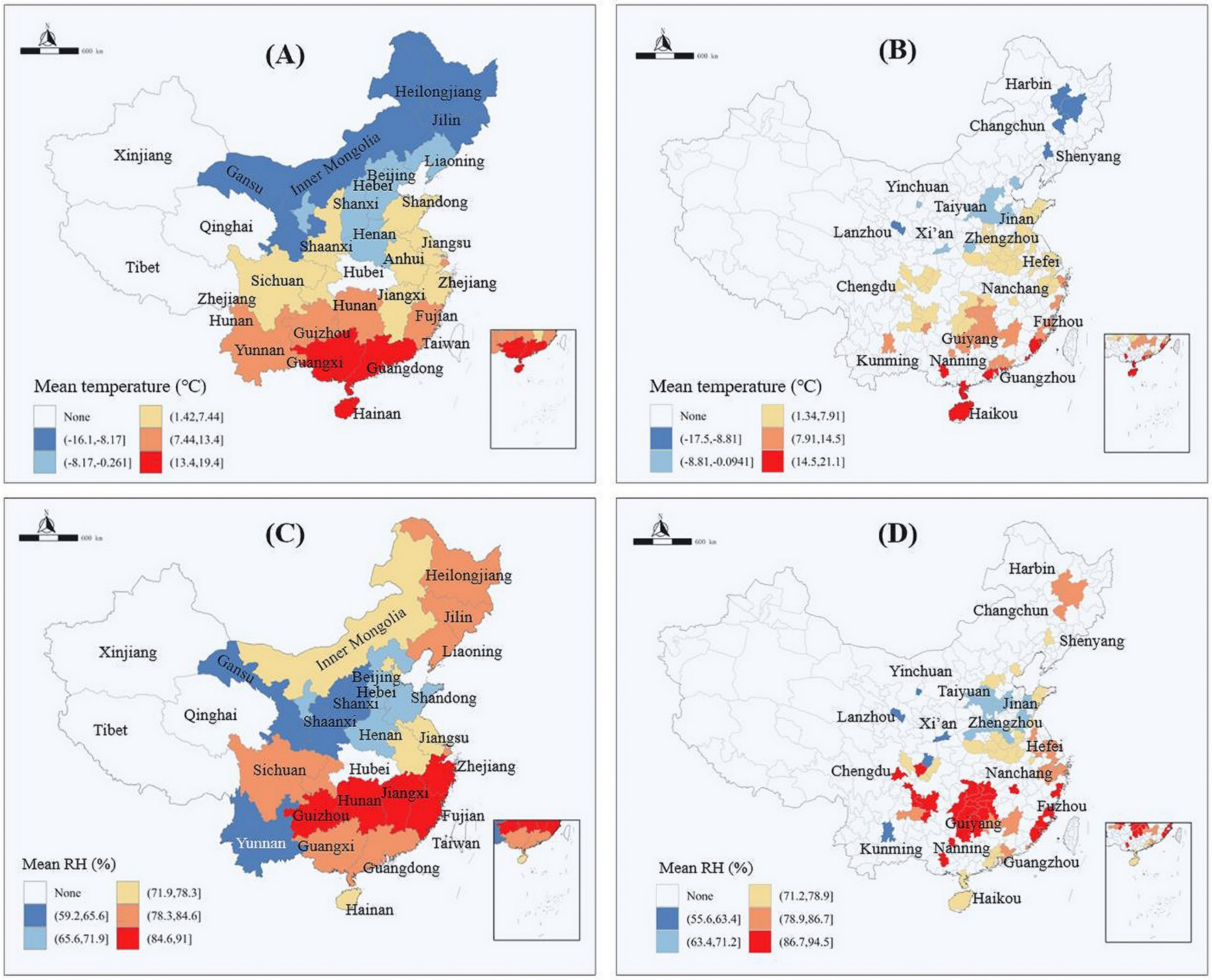

Figure S2. Geographic distributions of the average temperature in the province (A) and city (B) levels, and the average relative humidity in the province (C) and city (D) levels during Jan 14 – Feb 21, 2020. Only the large typical cities were marked.

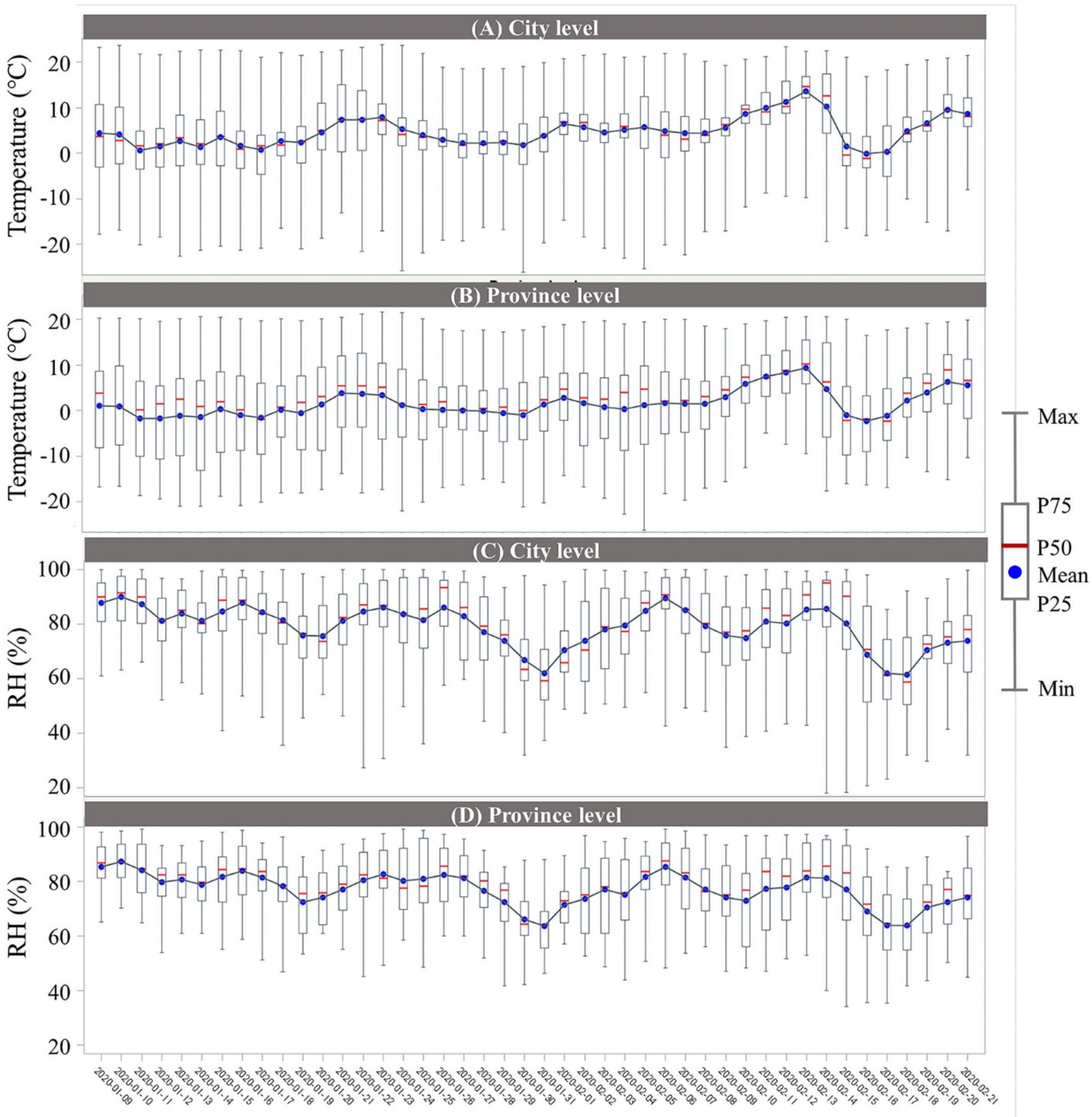

Figure S3. Distributions of the temperature in the city (A) and province (B) levels, and relative humidity in the city (C) and province (D) levels during Jan 14 – Feb 21, 2020. Data was shown with minimum (Min), maximum (Max), mean value (Mean), and 25%, 50%, and 75% percentiles, respectively.

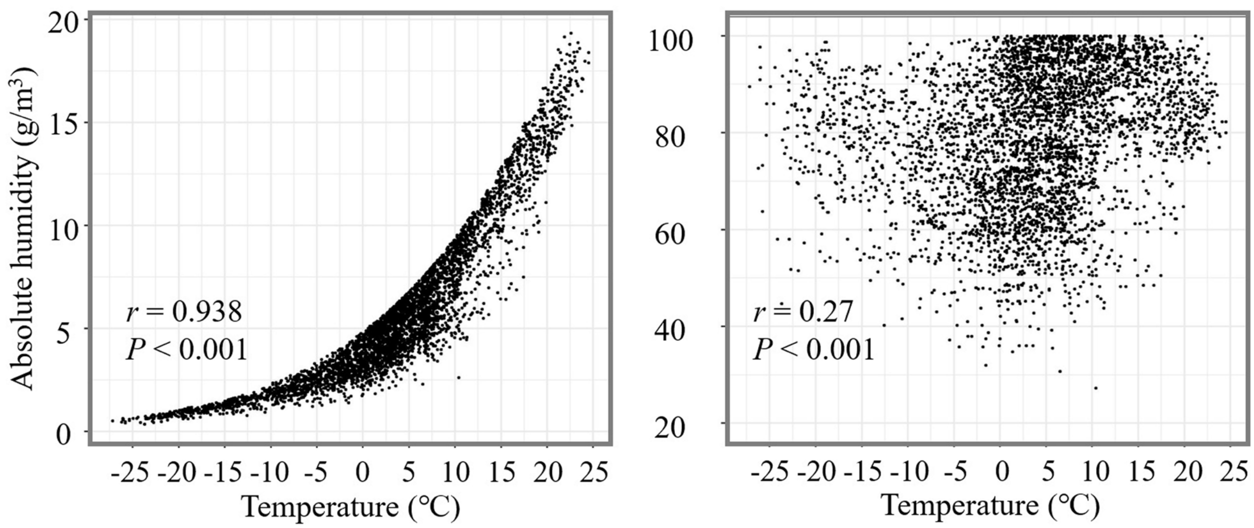

Figure S4. Scatter diagrams between the environmental temperature and absolute humidity (A) and relative humidity (B).

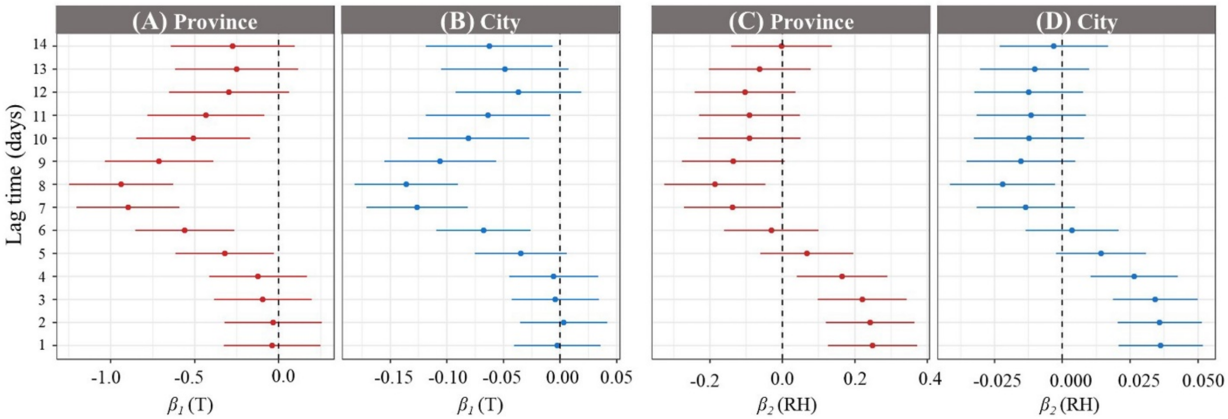

Figure S5. Associations of the ambient temperature (A: province level; B city level) and relative humidity (RH) (C: province; D: city) with the transmission rate of COVID-19 without adjusting for the mobility index, respectively. Transmission rate was defined as the increase rate of cumulated confirmed cases per-day in a logistic growth model (Eq. (1)). The regression coefficients (β_1 and β_2) were obtained using a linear mixed-effect model as the follows: $R_{[t,\, s]} = \beta_1 T_t + \beta_2 RH_t + \beta_3 WS_t + \beta_4 PR_t + \beta_5 PD_t + \gamma(L)$. This formula incorporated five fixed terms ($\beta_{1\text{-}5}$) to model the effects of temperature (T), relative humility (RH), wind speed (WS), precipitation (PR), population density (PD), and a random intercept (γ) to control for the location (L)-specific effects. Data was shown with the estimated value with 95% confidence interval.

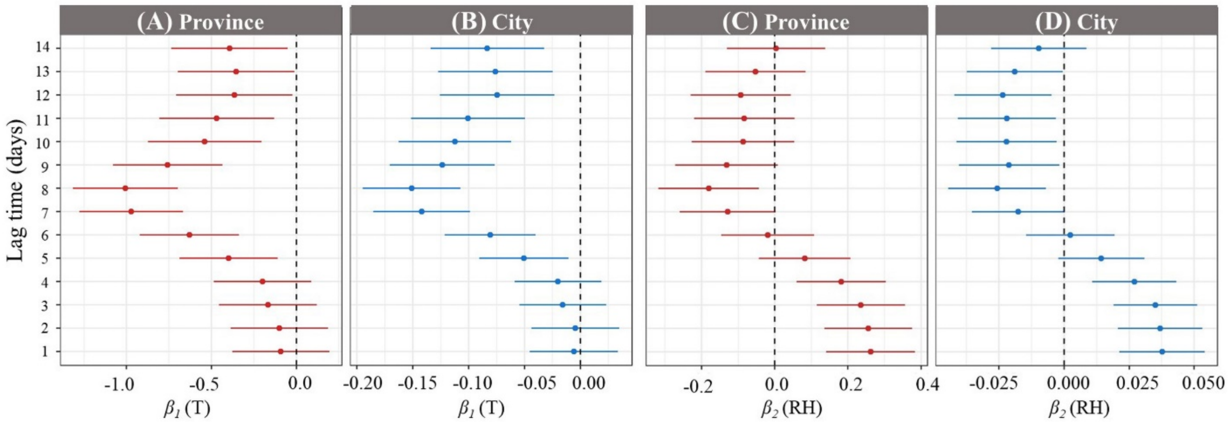

Figure S6. Associations of the ambient temperature (A: province level; B city level) and relative humidity (RH) (C: province level; D: city level) with the transmission rate of COVID-19 using the raw confirmed COVID-19 cases from the NHC website (not including the 200 infected cases in Rencheng Prison of Shandong Province, China), respectively. Transmission rate was defined as the increase rate of cumulated confirmed cases per-day in a logistic growth model (Eq. (1)). The regression coefficients (β_1 and β_2) were obtained using a linear mixed-effect model as the follows: $R_{[t,\ s]} = \beta_1 T_t + \beta_2 RH_t + \beta_3 WS_t + \beta_4 PR_t + \beta_5 MII_t + \beta_6 MOI_t + \beta_7 PD_t + \gamma(L)$. This incorporated seven fixed terms ($\beta_{1\text{-}7}$) to model the effects of temperature (T), relative humility (RH), wind speed (WS), precipitation (PR), population mobility indexes of moving-in (MII) and moving-out index (MOI), population density (PD), and a random intercept (γ) to control for the location (L)-specific effects. Data was shown with the estimated value with 95% confidence interval.

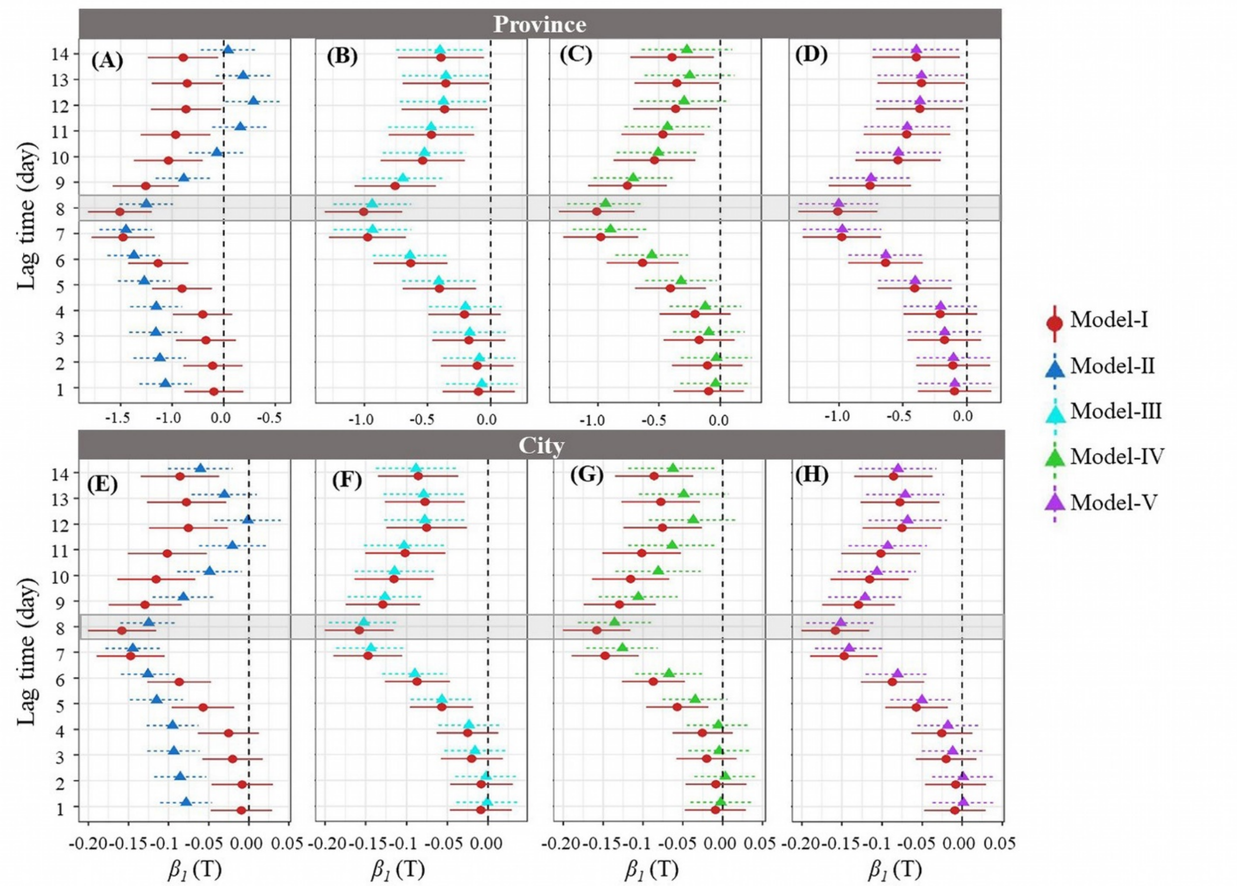

Figure S7. Associations of the ambient temperature (A-D: province level; E-H: city level) with the transmission rate of COVID-19 using the raw confirmed COVID-19 cases. Transmission rate was defined as the increase rate of cumulated confirmed cases per-day in a logistic growth model (Eq. (1)). The regression coefficient (β_1) was obtain using a linear mixed-effect model as the following models:

Model-I [All]: $R_{[t,\,s]} = \beta_1 T_t + \beta_2 RH_t + \beta_3 WS_t + \beta_4 PR_t + \beta_5 MII_t + \beta_6 MOI_t + \beta_7 PD_t + \gamma(L)$

Model-II [No PR]: $R_{[t,\,s]} = \beta_1 T_t + \beta_2 RH_t + \beta_3 WS_t + \beta_5 MII_t + \beta_6 MOI_t + \beta_7 PD_t + \gamma(L)$

Model-III [No WS]: $R_{[t,\,s]} = \beta_1 T_t + \beta_2 RH_t + \beta_4 PR_t + \beta_5 MII_t + \beta_6 MOI_t + \beta_7 PD_t + \gamma(L)$

Model-IV [No MII&MOI]: $R_{[t,\,s]} = \beta_1 T_t + \beta_2 RH_t + \beta_3 WS_t + \beta_4 PR_t + \beta_7 PD_t + \gamma(L)$

Model-V [No PD]: $R_{[t,\,s]} = \beta_1 T_t + \beta_2 RH_t + \beta_3 WS_t + \beta_4 PR_t + \beta_5 MII_t + \beta_6 MOI_t + \gamma(L)$

This incorporated seven fixed terms ($\beta_{1\text{-}7}$) to model the effects of temperature (T), relative humility (RH), wind speed (WS), precipitation (PR), population mobility indexes of moving-in (MII) and moving-out index (MOI), population density (PD), and a random intercept (γ) to control for the location (L)-specific effects. Data was shown with the estimated value with 95% confidence interval. The results at lag time = 8 days were highlighted by a gray rectangle.

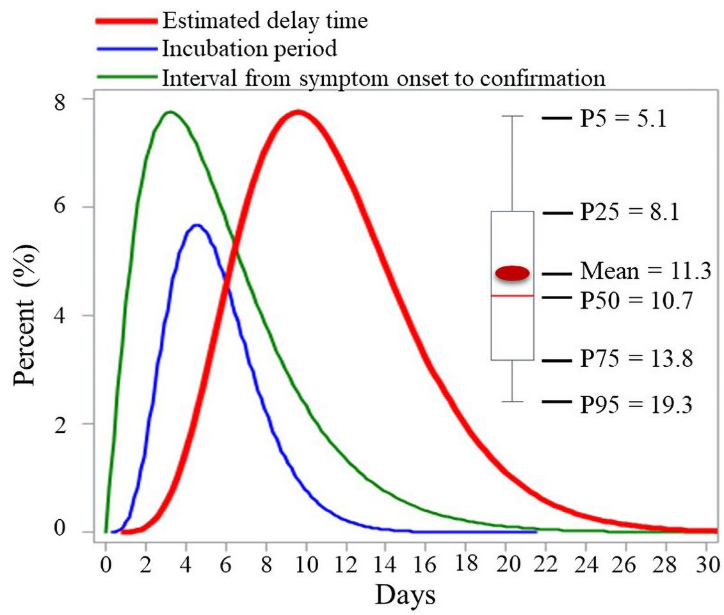

Figure S8. Distribution of the lag time including the incubation time and the interval between the symptom onset and the report of the COVID-19 case confirmation (report interval). The 5%, 25%, 50%, 75%, and 95% percentiles and mean value were 5.1, 8.1, 10.7, 13.8, 19.3, and 11.3 days. The distribution of incubation time and report interval both obey a Gamma distribution with the tuning parameters of (***a***=2.24, ***b***=2.59) [1] and (***a***=5.807, ***b***=0.948) [2], respectively.

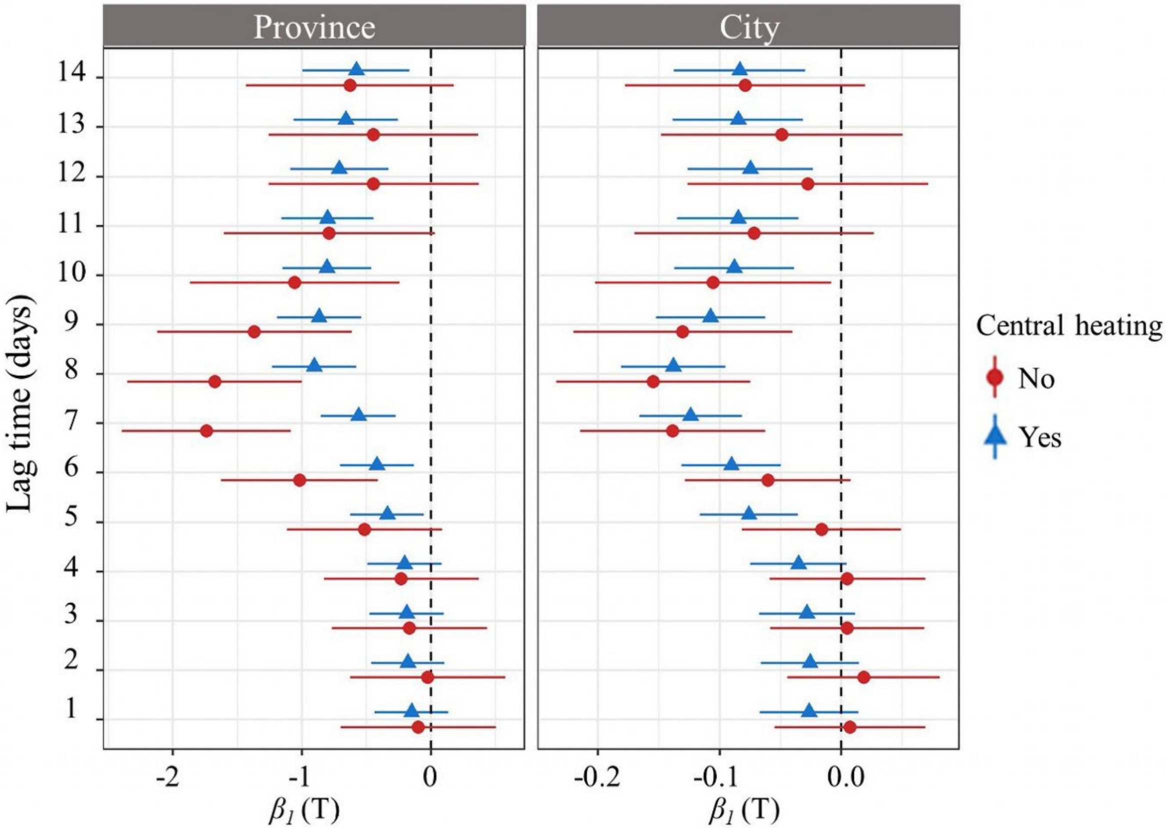

Figure S9. Modification effect of the central heating on the associations of the ambient temperature with the transmission rate of COVID-19 without adjusting for the mobility index in the province and city levels, respectively. Transmission rate was defined as the increase rate of cumulated confirmed cases per-day in a logistic growth model (Eq. (1)). The regression coefficient (β_1) was obtained using a linear mixed-effect model as the follows: $R_{[t,\ s]} = \beta_1 T_t + \beta_2 RH_t + \beta_3 WS_t + \beta_4 PR_t + \beta_5 PD_t + \gamma(L)$. This formula incorporated five fixed terms ($\beta_{1\text{-}5}$) to model the effects of temperature (T), relative humility (RH), wind speed (WS), precipitation (PR), population density (PD), and a random intercept (γ) to control for the location (L)-specific effects. Data was shown with the estimated value with 95% confidence interval.

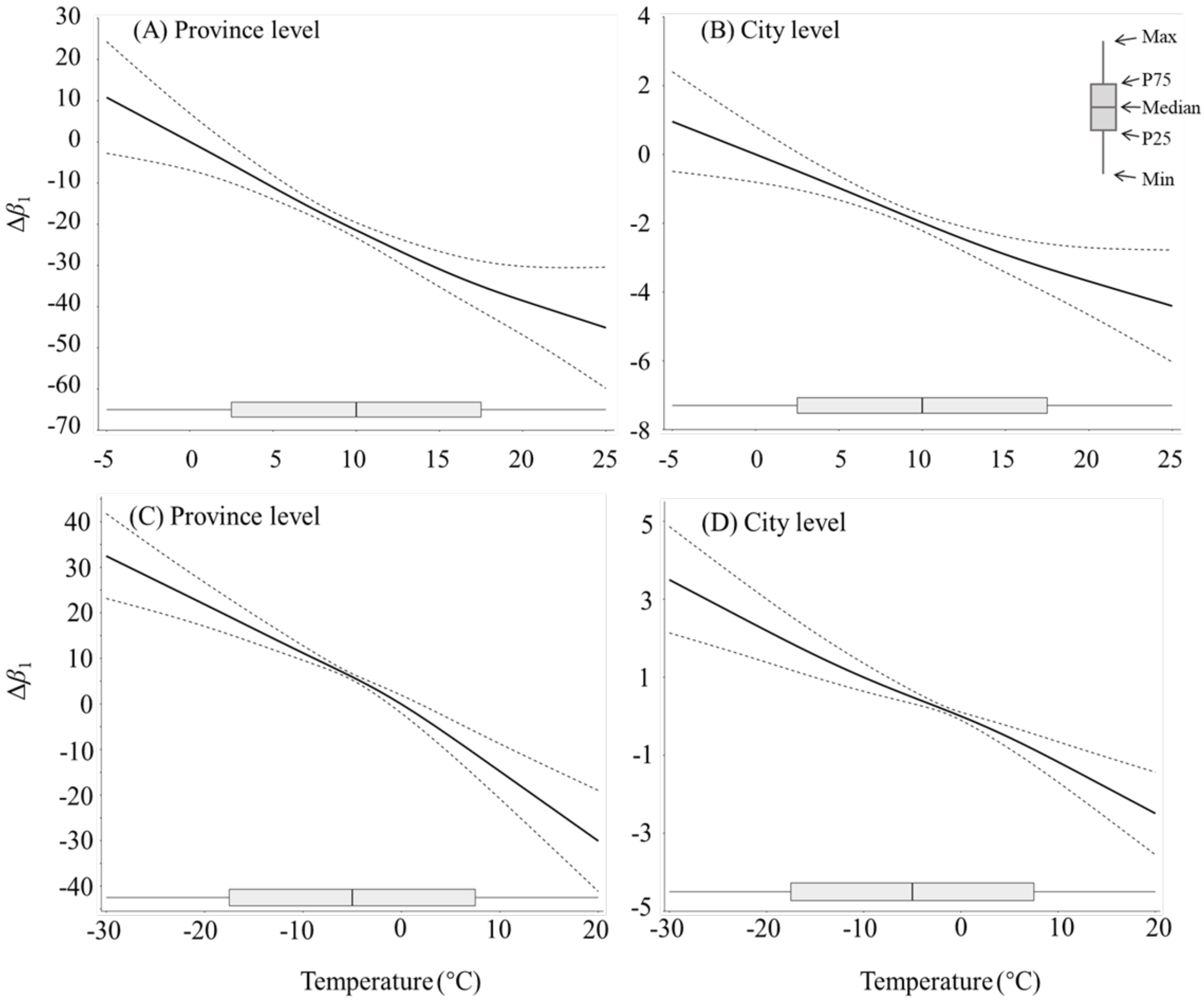

Figure S10. The non-linear relationship between ambient temperature and COVID-19 transmission when LT = 8 days among regions with (C&D) and without (A&B) central heating. Transmission rate was defined as the increase rate of cumulated confirmed cases per-day in a logistic growth model (Eq. (1)). The change of regression coefficient ($\Delta\beta_1$) was obtained using a non-linear mixed-effect model as the follows: $R_{[t,\, s]} = \boldsymbol{g}(T_t) + \beta_2 RH_t + \beta_3 WS_t + \beta_4 PR_t + \beta_5 MII_t + \beta_6 MOI_t + \beta_7 PD_t + \gamma(L)$. This formula incorporated a smoothing spline term (***g***), six fixed terms ($\beta_{2\text{-}7}$) to model the effects of temperature (*T*), relative humility (*RH*), wind speed (*WS*), precipitation (*PR*), population mobility indexes of moving-in (*MII*) and moving-out index (*MOI*), population density (*PD*), and a random intercept (γ) to control for the location (*L*)-specific effects. Solid and dot lines represented the estimation of $\Delta\beta_1$ and its 95% confidence interval, respectively. The reference value of temperature was 0°C. Box plots described the distribution of temperature during the period.

Table S1. Detailed data correction operation on the original information reported on the official website of the National Health Commission

Provinces	Events	Details	Correcting the reported data based on the event	Sources [a]
Tianjin	Baodi department store aggregation infection	Cluster of infection of 40 cases; No observed abnormal cumulated number	Keep unchanged.	Reference [3]
Shandong	Prison aggregation infection	Feb. 21, 2020: 200 new cases were confirmed in Rencheng prison	These 200 cases were deleted since 21st Feb, 2020	Website #1:
Zhejiang	Abnormal data	Jan. 31, 2020: "decreased" cumulated cases occurred	Corrected using the reported data from the Zhejiang Health Commissions official website	Website #2:
Zhejiang	Abnormal data in Hangzhou City	Feb. 9, 2020: "decreased" cumulated cases occurred	Kept unchanged. (Original data was consistent with Zhejiang Health Commissions official website	Website #3:
Gansu	Abnormal data in Gannan City	Jan. 21, 2020: "decreased" cumulated cases occurred	Corrected using the reported data from the Gansu Health Commissions official website	Website #4:
Henan	Abnormal data in Yongcheng City	Decreased cumulated cases occurred	Corrected using the reported data from the Henan Health Commissions official website	Website #5:
Heilongjiang	Abnormal data in Suihua City	Feb. 9, 2020: "decreased" cumulated cases occurred	Keep unchanged. (Original data was consistent with Heilongjiang Health Commissions official data)	Website #6:
Nanjing	Abnormal data	Decreased cumulated cases occurred	Corrected using the reported data from the Nanjing Health Commissions official website	Website #7:
Shaanxi	Abnormal data in Xian City	Feb. 2, 2020: "decreased" cumulated cases occurred	Corrected using the reported data from the Shaanxi Health Commissions official website	Website #8:
Sichuan	Abnormal data in Meishan city	Feb. 21, 2020: "decreased" cumulated cases occurred	Corrected using the reported data from the Sichuan Health Commissions official website	Website #9:
Yunnan	Abnormal data in Dali City	Decreased cumulated cases occurred	Corrected using the reported data from the Yunnan Health Commissions official website	Website #10:
Yunnan	abnormal data in Xishuangbanna City	Decreased cumulated cases occurred	Corrected using the reported data from the Yunnan Health Commissions official website	Website #11:

[a] The detailed websites:

Website #1: https://www.yicai.com/news/100515523.html

Website #2: http://www.zjwjw.gov.cn/art/2020/2/1/art_1202194_41865259.html

Website #3: http://www.zjwjw.gov.cn/art/2020/2/10/art_1202101_41894522.html

Website #4: http://wsjk.gansu.gov.cn/single/10910/84364.html

Website #5: http://hnwsjsw.gov.cn/channels/xxgk.shtml

Website #6: http://wsjkw.hlj.gov.cn/index.php/Home/Zwgk/show/newsid/7769/navid/42/stypeid/

Website #7: http://wjw.jiangsu.gov.cn/art/2020/2/5/art_7290_8961839.html

Website #8: http://sxwjw.shaanxi.gov.cn/art/2020/2/3/art_9_67666.html

Website #9: http://wsjkw.sc.gov.cn/

Website #10: http://ynswsjkw.yn.gov.cn/wjwWebsite/web/doc/UU158147060382734153

Website #11: http://ynswsjkw.yn.gov.cn/wjwWebsite/web/doc/UU158230893462979208

Table S3. The interaction effects between temperature and relative humidity on the transmission rate of COVID-19

Parameters [a]	Province level			City level		
	All [b]	Public heating status		All	Public heating status	
		No	Yes		No	Yes
T	-0.31 (-1.35~0.73)	-3.15 (-6.56~0.26)	-0.98 (-2.10~0.14)	-0.08 (-0.23~0.07)	-0.18 (-0.51~0.16)	-0.06 (-0.20~0.08)
RH	-0.19 (-0.33~-0.05)	-0.45 (-0.83~-0.07)	-0.20 (-0.37~-0.03)	-0.02 (-0.04~-0.002)	-0.02 (-0.06~0.01)	-0.04 (-0.06~-0.02)
$T \times RH$	-0.01 (-0.02~0.004)	0.02 (-0.02~0.05)	0.002 (-0.014~0.018)	-0.001 (-0.003~0.001)	-0.0001(-0.0039~0.0037)	-0.0008 (-0.028~0.0012)
P [c]	0.17	0.43	0.81	0.28	0.95	0.45

[a] Temperature (T) and relative humidity (RH);

[b] Including all the locations;

[c] Test for the interaction between the temperature and relative humidity using a linear mixed-effect model as the follows, $R_{[t, s]} = \beta_1 T_t + \beta_2 RH_t + \beta_3 WS + \beta_4 PR_t + \beta_5 MII_t + \beta_6 MOI_t + \beta_7 PD_t + \beta_8 T_t \times RH_t + \gamma(L)$, where The regression incorporated seven fixed terms ($\beta_{1\text{-}8}$) to model the effects of temperature (T), relative humility (RH), wind speed (WS), precipitation (PR), population mobility indexes of moving-in (MII) and moving-out index (MOI), population density (PD), the interaction between T and RH, and a random intercept to control for the location (L)-specific effects. A total 27 provinces and 99 cities were included when the lag time = 8 days

Table S4. The regression coefficients of temperature associated the transmission rate of COVID-19

Province name	City name	N [a]	β_1 [b]
Province level			
Henan	/	1267	-3.424
Anhui	/	988	-2.021
Hunan	/	1011	-1.955
Jiangxi	/	934	-1.944
Guangdong	/	1333	-1.924
Sichuan	/	525	-1.869
Jiangsu	/	631	-1.837
Zhejiang	/	1203	-1.714
Yunnan	/	174	-1.702
Shanghai	/	334	-1.691
Hainan	/	168	-1.681
Chongqing	/	567	-1.678
Guizhou	/	146	-1.611
Guangxi	/	246	-1.593
Fujian	/	293	-1.582
Heilongjiang	/	480	-1.075
Shandong	/	549	-1.054
Ningxia	/	71	-0.999
Shaanxi	/	245	-0.857
Beijing	/	396	-0.744
Tianjin	/	132	-0.654
Gansu	/	91	-0.641
Hebei	/	308	-0.619
Shanxi	/	132	-0.609
Inner Mongolia	/	75	-0.563
Jilin	/	91	-0.561
Liaoning	/	121	-0.367
City level			
Sichuan	Chengdu	143	-0.404
Guangdong	Shantou	25	-0.350
Hunan	Shaoyang	102	-0.333
Anhui	Fuyang	155	-0.328
Fujian	Xiamen	35	-0.321
Hunan	Yueyang	156	-0.305
Anhui	Liu'an	69	-0.262
Guizhou	Bijie	23	-0.259
Jiangsu	Wuxi	55	-0.253
Jiangsu	Suzhou	87	-0.253
Sichuan	Neijiang	22	-0.252
Guizhou	Guiyang	36	-0.248
Jiangsu	Changzhou	51	-0.241
Guangdong	Zhongshan	66	-0.239
Jiangsu	Nanjing	93	-0.237
Zhejiang	Jiaxing	45	-0.234
Hunan	Yiyang	59	-0.229

Province name	City name	N [a]	β_1 [b]
Hainan	Haikou	39	-0.227
Henan	Nanyang	155	-0.224
Anhui	Wuhu	33	-0.223
Sichuan	Mianyang	22	-0.222
Hunan	Loudi	76	-0.221
Henan	Zhengzhou	157	-0.216
Fujian	Zhangzhou	20	-0.216
Guangdong	Jiangmen	23	-0.215
Guangdong	Zhuhai	98	-0.212
Fujian	Fuzhou	71	-0.212
Anhui	Huainan	27	-0.207
Sichuan	Guang'an	30	-0.206
Anhui	Haozhou	108	-0.205
Anhui	Suzhou	41	-0.205
Yunnan	Kunming	53	-0.205
Zhejiang	Jinhua	55	-0.205
Zhejiang	Shaoxing	42	-0.204
Hunan	Changsha	242	-0.204
Anhui	Hefei	174	-0.202
Jiangsu	Nantong	40	-0.198
Sichuan	Luzhou	24	-0.196
Guangxi	Liuzhou	24	-0.194
Hunan	Xiangtan	35	-0.194
Jiangsu	Huai'an	66	-0.192
Guangdong	Shenzhen	416	-0.188
Sichuan	Dazhou	41	-0.187
Sichuan	Bazhong	24	-0.183
Hunan	Chenzhou	39	-0.174
Henan	Zhumadian	139	-0.174
Heilongjiang	Harbin	197	-0.173
Jiangsu	Taizhou	37	-0.173
Jiangsu	Xuzhou	79	-0.172
Hunan	Zhuzhou	78	-0.168
Hunan	Yongzhou	43	-0.168
Hebei	Tangshan	57	-0.166
Guizhou	Zunyi	32	-0.166
Henan	Shangqiu	91	-0.163
Sichuan	Nanchong	38	-0.161
Guangdong	Zhanjiang	22	-0.158
Guangdong	Dongwan	93	-0.157
Hunan	Huaihua	40	-0.157
Shandong	Yantai	47	-0.155
Zhejiang	Ningbo	157	-0.155
Hunan	Changde	80	-0.154
Guangxi	Nanning	54	-0.154
Jiangsu	Lianyungang	48	-0.153
Henan	Xinxiang	57	-0.152
Guangxi	Guilin	31	-0.150
Shandong	Weifang	44	-0.146

Province name	City name	N [a]	β_1 [b]
Anhui	Bengbu	160	-0.133
Henan	Zhoukou	76	-0.128
Shandong	Linyi	49	-0.124
Ningxia	Yinchuan	33	-0.123
Shandong	Liaocheng	38	-0.123
Henan	Kaifeng	26	-0.122
Hebei	Handan	31	-0.109
Shandong	Qingdao	59	-0.106
Guangdong	Huizhou	62	-0.104
Heilongjiang	Suihua	47	-0.104
Shandong	Dezhou	37	-0.101
Hunan	Hengyang	48	-0.099
Hebei	Xingtai	23	-0.099
Hebei	Baoding	32	-0.098
Shandong	Jinan	47	-0.093
Hebei	Langfang	30	-0.093
Guangdong	Foshan	84	-0.092
Hebei	Shijiazhuang	28	-0.091
Shaanxi	Xi'an	120	-0.088
Henan	Luoyang	31	-0.084
Gansu	Lanzhou	36	-0.082
Jiangxi	Ganzhou	76	-0.080
Henan	Xinyang	270	-0.063
Shanxi	Taiyuan	20	-0.061
Jilin	Changchun	45	-0.058
Liaoning	Shenyang	28	-0.038
Fujian	Quanzhou	46	-0.037
Zhejiang	Hangzhou	169	-0.016
Jiangxi	Nanchang	229	-0.004
Guangdong	Guangzhou	339	0.004
Zhejiang	Wenzhou	504	0.665

[a] Number of subjects;

[b] The regression coefficient (β_1) was obtain using a linear mixed effect model as the follows: $R_{[t,\ s]} = \beta_1 T_t+\beta_2 RH_t+\beta_3 WS+\beta_4 PR_t+\beta_5 MII_t+\beta_6 MOI_t+\beta_7 PD_t+ (T_t|\gamma(L))$. This incorporated seven fixed terms ($\beta_{1\text{-}7}$) to model the effects of temperature (T), relative humility (RH), wind speed (WS), precipitation (PR), population mobility indexes of moving-in (MII) and moving-out index (MOI), population density (PD), a random slope of temperature (T), and a random intercept (γ) to control for the location (L)-specific effects. A total 27 provinces and 99 cities were included when the lag time = 8 days.

Table S5. The accumulated number of COVID-19 cases associated with the increase of ambient temperature during the *D* days at different lag time.

Lag time (Day)	ΔN_M [a] (95% Confidence Interval)
1	-38.2 (-193.2, 116.8)
2	-21.6 (-142.2, 99.1)
3	-121.2 (-387.7, 145.3)
4	-306.4 (-820.8, 208.1)
5	-840.1 (-1605.4, -74.8)
6	-2216.3 (-3367.0, -1065.6)
7	-4177.7 (-5589.5, -2765.9)
8	-4066.6 (-5553.8, -2579.3)
9	-3181.5 (-4798.6, -1564.3)
10	-1882.2 (-3192.5, -571.9)
11	-1010.3 (-1933.2, -87.4)
12	-619.3 (-1459.5, 221.0)
13	-530.4 (-1206.9, 146.1)
14	-569.3 (-1126.9, -11.7)

[a] ΔN_M: The accumulated number of COVID-19 cases associated with the increase of ambient temperature during the D days. Negative values represent decreased number of associated cases were estimated.

Table S6. Stability of SARS-CoV-2 at different environmental conditions and their half times of decay

Incubation time/ hours	Experimental conditions							
	4℃		20℃		28℃		37℃	
	L	H	L	H	L	H	L	H
	Mean value							
0	37000	37000	37000	37000	37000	37000	37000	37000
1	18000	33000	28000	18500	38500	17000	2310	7750
4	8000	18500	18500	3450	1120	725	755	200
8	12000	13500	12000	15000	4450	4100	25	40
24	5900	22500	2900	3000	105	/	/	/
48	12000	11500	225	/	/	/	/	/
72	3250	20000	/	/	/	/	/	/
	Standard deviation							
0	8485	8485	8485	8485	8485	8485	8485	8485
1	8485	9899	5657	3536	10607	2828	1824	71
4	1414	4950	707	636	1386	672	21	283
8	2828	2121	0	2828	71	141	21	14
24	566	7778	283	1414	35	/	/	/
48	2828	4950	106	/	/	/	/	/
72	1485	5657	/	/	/	/	/	/
	Half time [a]							
Estimated	1.97	3.89	4.28	1.19	0.61	0.65	0.85	0.36
95%CI_L	1.18	2.06	2.54	0.98	0.36	0.47	0.43	0.21
95%CI_U	6.06	33.00	13.52	1.50	1.86	1.03	28.72	1.44

[a] The half time of decay was estimated by assuming the first-order decay trend using the first 4-hour residual titers. 95%CI_L and 95%CI_U stand for the low and upper limits of the 95% confidence interval.

Table S2: The increasing trend of the confirmed COVID-19 cases during Jan. 23–Feb. 21, 2020 and their fitting parameters using a Logistic model for the selected 27 provinces and 99 cities.

Data S1. The data of daily increased COVID-19 cases with and without corrections from the NHC website report

Data S2. Human mobility index used to indicate of the individual movement among the concerned provinces or cities in our study. Sourced from the Baidu Co. service (see the website: http://qianxi.baidu.com/)

Data S3. The information of the temperature and relative humidity of the concerned area during the study period.

Reference

1. Guan, W. J.; Ni, Z. Y.; Hu, Y., et al., Clinical Characteristics of Coronavirus Disease 2019 in China. *N Engl J Med* **2020,** *382*, (18), 1708-1720, https://www.nejm.org/doi/10.1056/NEJMoa2002032.
2. Lauer, S. A.; Grantz, K. H.; Bi, Q., et al., The Incubation Period of Coronavirus Disease 2019 (COVID-19) From Publicly Reported Confirmed Cases: Estimation and Application. *Ann Intern Med* **2020,** *172*, (9), 577-582, https://doi.org/10.7326/M20-0504.
3. Wu, W. S.; Li, Y. G.; Wei, Z. F., et al., [Investigation and analysis on characteristics of a cluster of COVID-19 associated with exposure in a department store in Tianjin]. *Chin J of Epi* **2020,** *41*, (4), 489-493, https://pubmed.ncbi.nlm.nih.gov/32133830.